

Lawrence Berkeley National Laboratory

Lawrence Berkeley National Laboratory

Title

DESULFURIZATION OF COAL MODEL COMPOUNDS AND COAL LIQUIDS

Permalink

<https://escholarship.org/uc/item/7984c9mf>

Author

Wrathall, James Anthony

Publication Date

1979-04-01



Lawrence Berkeley Laboratory

UNIVERSITY OF CALIFORNIA

ENERGY & ENVIRONMENT DIVISION

DESULFURIZATION OF COAL MODEL COMPOUNDS AND COAL LIQUIDS

James Anthony Wrathall* and Eugene E. Petersen

April 1979

*Filed as a M. S. thesis ✓

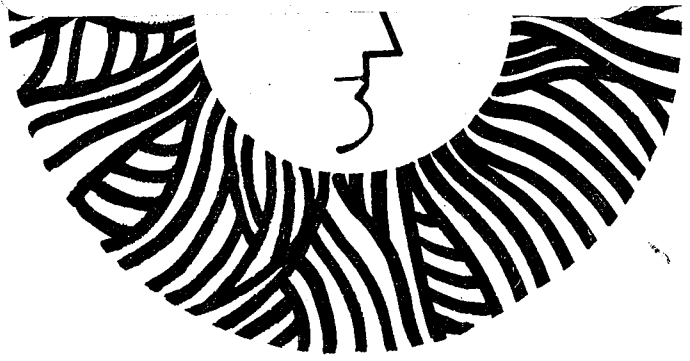
LA
CD
OSTI pdf
RCO
Scan

7
This is
which
For a
Tech.
eeks.

RECEIVED
LAWRENCE
BERKELEY LABORATORY

AUG 28 1979

LIBRARY AND
DOCUMENTS SECTION



LBL-8576 c. 2

1944

1945

1946

1947

f work
Neither
rtment
of their
loyees,
sumes
uracy,
ation,
esents
ights.

CONTENTS

FIGURE CAPTIONS	iv
LIST OF TABLES.	vi
ABSTRACT.	viii
I. INTRODUCTION.	1
A. Atmospheric Pollutants Associated With Coal Combustion. . .	1
B. E.P.A. Control Guidelines for Coal-Derived Pollutants . . .	3
C. Forms of Sulfur in Coal	8
D. Coal Desulfurization Processes.	11
E. Applicability of Cleaning Processes to U. S. Coals.	21
F. Objectives of This Study.	24
G. Chemistry of Model Compounds.	24
H. Chemistry of Sodium	26
II. EXPERIMENTAL.	32
A. Apparatus	32
B. Chemicals	34
C. Analyses.	35
III. RESULTS AND DISCUSSION.	40
A. Model Compounds	40
B. Mechanism of Dibenzothiophene Desulfurization	46
C. Coal and Coal-Derived Materials	65
IV. APPLICATIONS.	70
A. Modified SRC Process.	70
B. Modified SRC Process Economics.	77
C. Co-Combustion Process for Coal Cleaning	79
V. CONCLUSIONS	87
VI. ACKNOWLEDGEMENTS.	88
VII. REFERENCES.	89

FIGURES	Page
1. Nitrogen oxide control	7
2. Sulfur compound distribution in petroleum feedstock	12
3. Model compounds representative of coal sulfur species	13
4. Hydrodesulfurization thermodynamics of coal sulfur	14
5. K-T gasification process	19
6. SRC I process	20
7. U. S. coal cleanability	23
8. Desulfurization and hydrogenation reactions of sodium	30
9. Mass balance for SRC sulfur distribution	38
10. Dibenzothiophene desulfurization vs. molar Na/S	41
11. Dibenzothiophene desulfurization vs. time	42
12. Thianthrene desulfurization vs. time	43
13. Benzothiophene desulfurization vs. time	44
14. Diphenyl sulfide desulfurization vs. time	45
15. Reserpine K-curve	47
16. Hydrogen-char VPO curve	48
17. Nitrogen-char VPO curve	49
18. Sternberg's mechanism of dibenzothiophene desulfurization	51
19. Calculated vs. experimental curves of dibenzothiophene concentration vs. time	53
20. Rate of biphenyl formation vs. time	54
21. Proposed mechanism of dibenzothiophene desulfurization	60
22. Calculated vs. experimental curves of radical anion concentration vs. time	62

	Page
23. Rate of dibenzothiophene reaction vs. hydrogen pressure	64
24. Modified SRC process	71
25. SRC II mass flows	72
26. SRC II atmospheric bottoms flows	73
27. Modified process atmospheric bottoms flows	74
28. Co-combustion process	81

LIST OF TABLES		Page
1.	Results of Epidemiological Studies	2
2.	U. S. Manmade SO ₂ Emissions, 1972 ^a	4
3.	Calculation of SO ₂ Production from Two Coals	6
4.	Sulfur Distribution in some U. S. Coals.	9
5.	Physical Coal Cleaning Process Efficiencies.	15
6.	Description of Chemical Coal Cleaning Processes.	17
7.	Sulfur Removal in Coal Conversion Processes.	18
8.	Technically Feasible Flue-Gas Operations	22
9.	Coal Reserve Cleanability, B.O.M. Data*	25
10.	Methods Studied for Desulfurization of Model Compounds	27
11.	Organic Reactions of Sodium.	28
12.	Experimental Chemicals	33
13.	Ultimate Analyses of Coal-related Materials.	34
14.	Feed Coal and Product SRC Composition.	35
15.	Calculation of Experimental Curve of Dibenzothiophene Concentration vs. Time	52
16.	Calculation of Radical Anion Concentration vs. Time Mechanism I	58
16A.	Calculation of Radical Anion Concentration vs. Time Mechanism II.	61
17.	Experimental Values Used in Calculations	65
18.	Reaction of Solid SRC and Coal with Sodium	66
19.	Sulfur Distribution Resulting from Reaction of Sodium with SRC Recycle Slurry.	68
20.	Vapor-Liquid Distribution Resulting from Reaction of Sodium with SRC Recycle Slurry	68
21.	Average Values of Sulfur and Vapor-Liquid Distribution	69

	Page
22. Sulfate Salt Decomposition Temperatures	75
23. Relative Volatilities of Reactants and Products in Hydrodesulfurization Reactions	76
24. Flue Gas Scrubbing Costs.	78
25. Changes in SRC Economics Due to Sodium Treatment.	78
26. Effect of Sulfur Content on Fuel Oil Value.	79
26A. Sulfur Retention by Sodium Salts.	82
27. Operating Costs, 1979 \$/Ton Coal.	83
28. Installed Costs, 1979 10^6 \$, 10^4 ton/day Capacity.	83
29. Chemical Coal Cleaning Costs.	84

4
40

DESULFURIZATION OF COAL MODEL COMPOUNDS AND COAL LIQUIDS

James Anthony Wrathall

Lawrence Berkeley Laboratory
University of California
Berkeley, CA 94720

ABSTRACT

Most U. S. coals contain sulfur concentrations that prevent their being burned without some form of sulfur removal. Current coal-cleaning technology can only remove the fairly reactive pyritic (inorganic) and aliphatic (organic) sulfur. A process which removes the more refractory hetero-aromatic sulfur can substantially increase the amount of coal reserves amenable to chemical cleaning.

Sodium metal dispersions convert refractory model compounds into lighter desulfurized products and non-volatile sulfur-rich char. When treated with sodium, coal-derived solids show substantial desulfurization. The same treatment applied to coal-derived liquids, when combined with vacuum distillation of the reaction product, yields a desulfurized light distillate, an increase in absolute amount of distillate, and retention of sulfur in the vacuum residue. The presence of sodium in the residue allows fixation of the residual sulfur as Na_2SO_4 upon combustion, eliminating production of SO_2 in the flue gas.

Intimate contacting of sodium salts with high sulfur coal also fixes 97-99% of the sulfur as Na_2SO_4 upon combustion. This technique takes advantage of the high energy available for carbon-sulfur bond cleavage during combustion and the reaction of SO_2 to form Na_2SO_4 to provide an inexpensive method for complete coal desulfurization.

I. INTRODUCTION

In order to justify expensive desulfurization programs, the deleterious effects of SO_2 and related pollutants are reviewed.

A. Atmospheric Pollutants Associated With Coal Combustion

Sulfur oxides, nitrogen oxides, and particulate matter are the chief atmospheric pollutants resulting from coal combustion. Their impact on the environment is reviewed below.

Sulfur dioxide is the principal product of sulfur combustion in power plants. SO_2 alone is a mild irritant (1), and may be carcinogenic in combination with fly-ash aromatics such as benzo-(a)-pyrene (2). In addition, crops show leaf damage and reduced growth upon SO_2 deposition (3).

Sulfuric acid (H_2SO_4) and SO_3 are the chief derivatives of atmospheric SO_2 . Health effects associated with these compounds are much more severe. They include increased asthma frequency, cardio-pulmonary aggravation, decreased ventilation efficiency in old and young alike, and generally higher morbidity in women, children, and the aged (1,4). Health effects are reviewed in Table 1.

Economic factors resulting from SO_x pollution include crop, ecological, and materials damage amounting to \$20 million per microgram per meter³ per year (3) (about \$160 million per year in the heavily industrialized Northeast) (1). Other less tangible effects include reduced visibility and acid rain (1).

Table 1 - Results of Epidemiological Studies

Adverse health effect	Concentration ^a at which effect was observed		Averaging time
	SO ₂ , µg/m ³ (ppm)	Sulfates, µg/m ³	
Increased mortality	300-400 (0.11-0.15)	NA ^b	24 hr
Aggravation of symptoms in elderly	365 (0.14)	8-10	24 hr
Aggravation of asthma	180-250 (0.07-0.09)	6-10	24 hr
Decreased lung function in children	220 (0.075)	11	Annual mean
Increased acute lower respiratory disease in families	90-100 (0.034-0.037)	9	Annual mean
Increased prevalence of chronic bronchitis	95 (0.035)	14	Annual mean
Increased acute respiratory disease in families	106 (0.039)	15	Annual mean
Increased respiratory disease related illness absences in female workers		13	Annual mean
Primary standard	365	-	24 hr
Primary standard	80	-	Annual mean

^aEffects levels are best judgment estimates based on a synthesis of several studies.

^bNA = not available.

From EPA Position Paper on Regulation of Atmospheric Sulfates (Reference 1.).

Power plants are the major sources of SO_2 ; point sources give twenty-five times natural emissions in highly urbanized regions. Serious air transport problems also result from taller stacks, which give SO_x a much longer air residence time (1,5). SO_2 sources are reviewed in Table 2.

Quantitative health effects of SO_x are poorly known, but EPA estimates that chronic annual averages of $10\text{--}15 \mu\text{g}/\text{m}^3$ and maximum daily doses of $6\text{--}10 \mu\text{g}/\text{m}^3$ are tolerable (1).

Nitrogen oxides show their effects mainly in combination with oxidizing organic species (e.g., PAN or smog, which is also known as peroxy-acetyl nitrate (2). PAN is shown to be an eye irritant, an asthma inducer, and a factor in generally decreased pulmonary function.

The effects of particulates in stack gas are also poorly known. Fly ash containing benzo-(a)-pyrenes is shown to be carcinogenic, and promoted by SO_2 (2,4).

All these hazardous materials must be effectively controlled at safe levels agreed upon by the EPA and industry.

B. E.P.A. Control Guidelines for Coal-Derived Pollutants

The currently proposed* EPA guidelines for SO_2 emissions are 1.2 pounds SO_2 per million BTU heat input of solid fuel, and 0.8 pounds per million BTU liquid fuel input. Uncontrolled emissions must now achieve 85% control, unless this results in less than 0.2 pounds SO_2 per million

* As of September, 1978; new proposal is $0.5 \text{ lbSO}_2/\text{BTU}$ for either fuel.

Table 2 - U. S. Manmade SO₂ Emissions, 1972^a

Source	Emissions 10 ⁶ tons	% of total emissions
Stationary fuel combustion ^b		77
Electric utilities ^b	18.0	55
Coal	16.5	
Oil	1.5	
Industrial/commercial (point sources)	3.6	11
Coal	2.5	
Oil	1.0	
Other	0.1	
Area sources	3.5	11
Industrial processes		21
Transportation		1.8
Automotive	0.2	0.6
Other	0.4	1.2
Solid waste		0.3
Miscellaneous		0.3
Total, all sources	32.7	100

^aNEDS data.²⁵

^bSASD data file.

From EPA Position Paper (Ref. 1).

BTU heat input. These figures are based on typical flue-gas desulfurization efficiencies of 85 to 95% (6).

As an example, if moisture-free Illinois #6 coal (at 5.0% S) is burned, 8.3 pound SO_2 per million BTU results, requiring 85% sulfur removal. On the other hand, a lignite with 0.8% moisture-free sulfur will produce 2.0 pounds SO_2 per million BTU. 90% removal will result in the EPA's lower bound on SO_2 emission, which is 0.2 pounds SO_2 per million BTU. Sample calculations of these figures are shown in Table 3.

As a possible incentive to other desulfurization technologies, EPA states that physical-chemical coal cleaning, SO_4 fixation in slag or bottom ash, coal gasification, or coal liquefaction can be used to achieve uncontrolled emission reduction of 85%, as long as emissions remain within the boundary of the standards referred to above.

Limits for NO_x emission are similar in magnitude to those for SO_2 emission. 0.5 pound NO_x is allowed for lignite or liquid fuels, while 0.6 pound NO_x is allowed for bituminous coal. These limits are based on those attainable by careful control of combustion, proper burner design and reduction of both flame temperature and O_2 -to-fuel ratio (6,7,8).

Figure 1 illustrates an example of NO_x control. The process is a coal-fired furnace used to heat a coal-solvent slurry up to the temperature required for hydrogenation. The furnace uses no excess O_2 and a 1:1 flue gas recycle to air feed ratio. Under these conditions, the slurry is heated to 470° C and the furnace gas temperature remains

Table 3 - Calculation of SO₂ Production from Two Coals

Illinois #6 Coal	$\frac{0.05 \text{ lb. S}}{\text{lb. Mf Coal}} \times \frac{1 \text{ lb. Coal}}{12 \text{ MBTU}} \times \frac{10^3 \text{ MBTU}}{\text{MMBTU}} \times \frac{2 \text{ lb. SO}_2}{\text{lb. S}} = \frac{8.3 \text{ lb.}}{\text{MMBTU}}$
Wyodak Coal	$\frac{0.008 \text{ Lb.}}{\text{lb. Mf Coal}} \times \frac{1 \text{ lb. Coal}}{8 \text{ MBTU}} \times \frac{10^3 \text{ MBTU}}{\text{MMBTU}} \times \frac{2 \text{ lb. SO}_2}{\text{lb. S}} = \frac{2.0 \text{ lb.}}{\text{MMBTU}}$

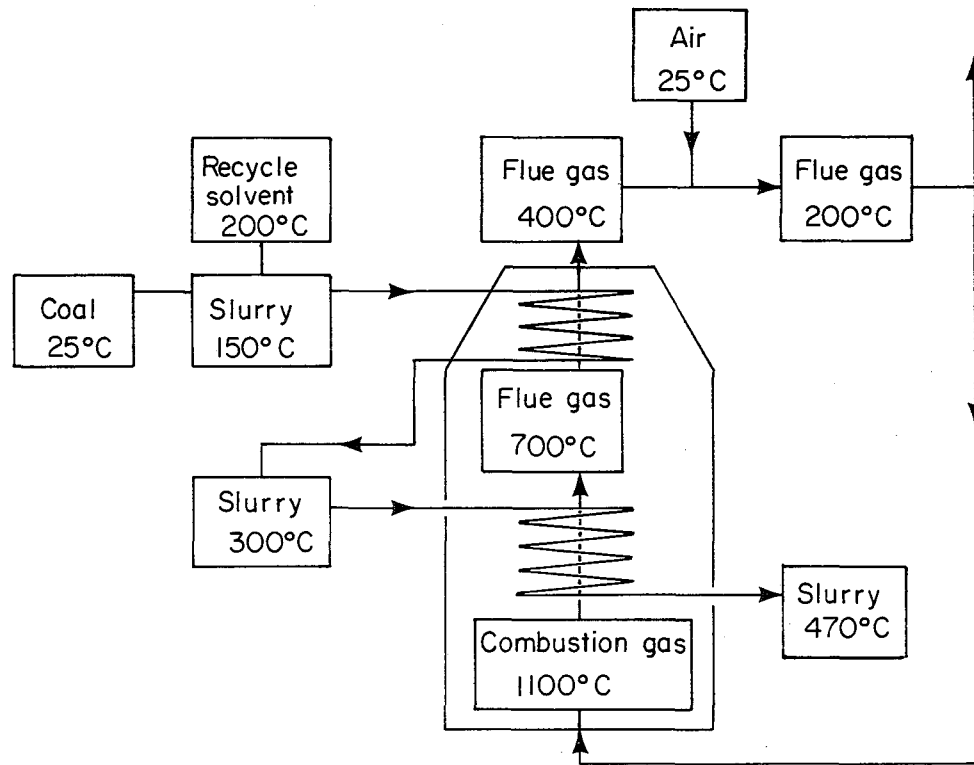


Fig. 1 Nitrogen oxide control

XBL 795-1510

below 1100° C. This temperature, in combination with the partial pressure of N₂, gives an equilibrium partial pressure of NO equivalent to the lower of the two EPA NO_x standards (9,10).

EPA proposes 0.03 pound particulates per million BTU input. This is based on a 99% reduction for most solid fuels, a 70% reduction for liquid fuels, and 0% for gaseous fuels. Best available baghouse (low-ash) or electro-static precipitator (high-ash) technology is assumed. Wet scrubber or combination flue-gas desulfurization-deashing is not considered in these limits, due to problems such as mist entrainment and clogging. Industry requests 0.08 pound per million BTU limit, so the status of the above limit is in doubt (6).

C. Forms of Sulfur in Coal

Design of desulfurization processes is dependent on the form of sulfur to be removed, so it is important to review the nature of sulfur in coal.

Sulfur appears in both organic and inorganic forms. The latter is composed of pyrite, pyrrhotite, sulfate, and elemental sulfur, in that order of abundance (11,12). Pyrite is usually the chief inorganic sulfur species (13), and sulfates are important only in weathered coals (11,14). In addition, forms such as sphalerite (ZnS), chalcopyrite (CuFeS_x), and galena (PbS) occur, leading to errors in pyritic sulfur determination (14). The mean inorganic to organic sulfur ratio for many U. S. coals is 1.56 (13,16).

Table 4 gives sulfur distribution for a number of coals.

Table 4 - Sulfur Distribution in some U. S. Coals

Sample	Sulfur (%)				Ash (%)
	Total	pyritic	Sulfate	Organic	
719-2 (Ohio)	6.3	1.58	2.74	1.9	14.2
719-3 (Ohio)	5.2	3.6	0.07	1.4	17.1
Hazard #4 (Kentucky)	1.52	0.66	0.04	0.82	12.8
Colstrip #2 (Western)	0.68	0.18	0.14	0.36	9.0
Beach Bottom #1 (W. Va.)	1.97	1.35	0.03	0.59	25.1

'from Paris, "Organic Sulfur", in Wheelock, Coal Desulfurization, Ref. 14.

Coal	Total Sulfur	Inorganic Sulfur	Organic Sulfur	% Ash
Indiana V (Warrick Co.)	4.63	2.44	2.19	12.8
Indiana VI (Warrick Co.)	4.17	2.20	1.97	11.4
Illinois V (Wabash Co.)	3.59	2.39	1.20	10.3
Illinois VI (Williamson Co.)	1.98	1.02	0.96	7.1

From Murray, "Magnetic Desulfurization", in Wheelock (Ref. 17)

Reactive organic sulfur is given that name due to its relative ease of hydro-desulfurization and pyrolytic desulfurization (18,19,20). Examples of these sub-units are mercaptans, aliphatic sulfides, and disulfides, which are shown to exist in coal by iso-octane extraction (21). The occurrence of these compounds, analogous with their more stable (22) oxygen counterparts, is predicted by both Hill and Lyon (23) and by Wiser (24).

Also predicted by Wiser, Hill and Lyon are hetero-aromatic compounds with sulfur present in thiophenic form (25). These compounds can also be called residual sulfur due to their generally high boiling points and molecular weights (26,27). Thiophene has been isolated from coal tar as a product of low-temperature pyrolysis (28,29). Thianaphthenes' (benzothiophenes') existence in coal tar was shown by Boes (30) and Weissgerber (31), and Weissgerber concluded that all the coal tar sulfur is thiophenic (32). Impure phenanthrene and fluorene, both coal-derived molecules, yield dibenzothiophene (33), which also results from aniline extraction of coal-derived bitumen (34). Dibenzothiophene is also found in Mideast gas oil (35). In addition, dibenzothiophene, benzothiophene, diphenyl sulfide, and various other thiophene derivatives are found in iso-octane extraction of Turkish coals (21). Lewis acids form thianthrene from diphenyl sulfide, which has been designated a coal subunit by various authors (36,37,38). Other studies show that dibenzothiophene and benzothiophene carboxylic acids

result from chromic-acid-treated coal (39,40). Figure 2 illustrates the relative amounts of reactive and refractory sulfur in a gasoline feedstock, while Figure 3 illustrates the structure of the various refractory compounds referred to above.

The term "refractory" is applied to the four compounds illustrated in Figure 3 based on their thermodynamics of hydro-desulfurization. Equilibrium constants for the hydro-desulfurization of a number of model compounds are compared in Figure 4 (41,42). Activation energies are unknown in most cases.

D. Coal Desulfurization Processes

Coal can be desulfurized prior to, during, or after combustion. Desulfurization prior to combustion can be divided into three categories: physical removal, extraction and leaching, and gas-solid reaction (43). Desulfurization during combustion involves sulfate fixation in ash or slag. Post-combustion desulfurization is also known as flue-gas scrubbing.

Pre-Combustion Cleaning

Physical processes consist of pyrite removal. They depend on differences in properties of pyrite and organic material: differing density, wettability, and para-magnetism. Since pyrite accounts for 50% or more of many coals' sulfur, some form of physical treatment is usually advisable (44,45). Several physical processes are summarized in Table 5.

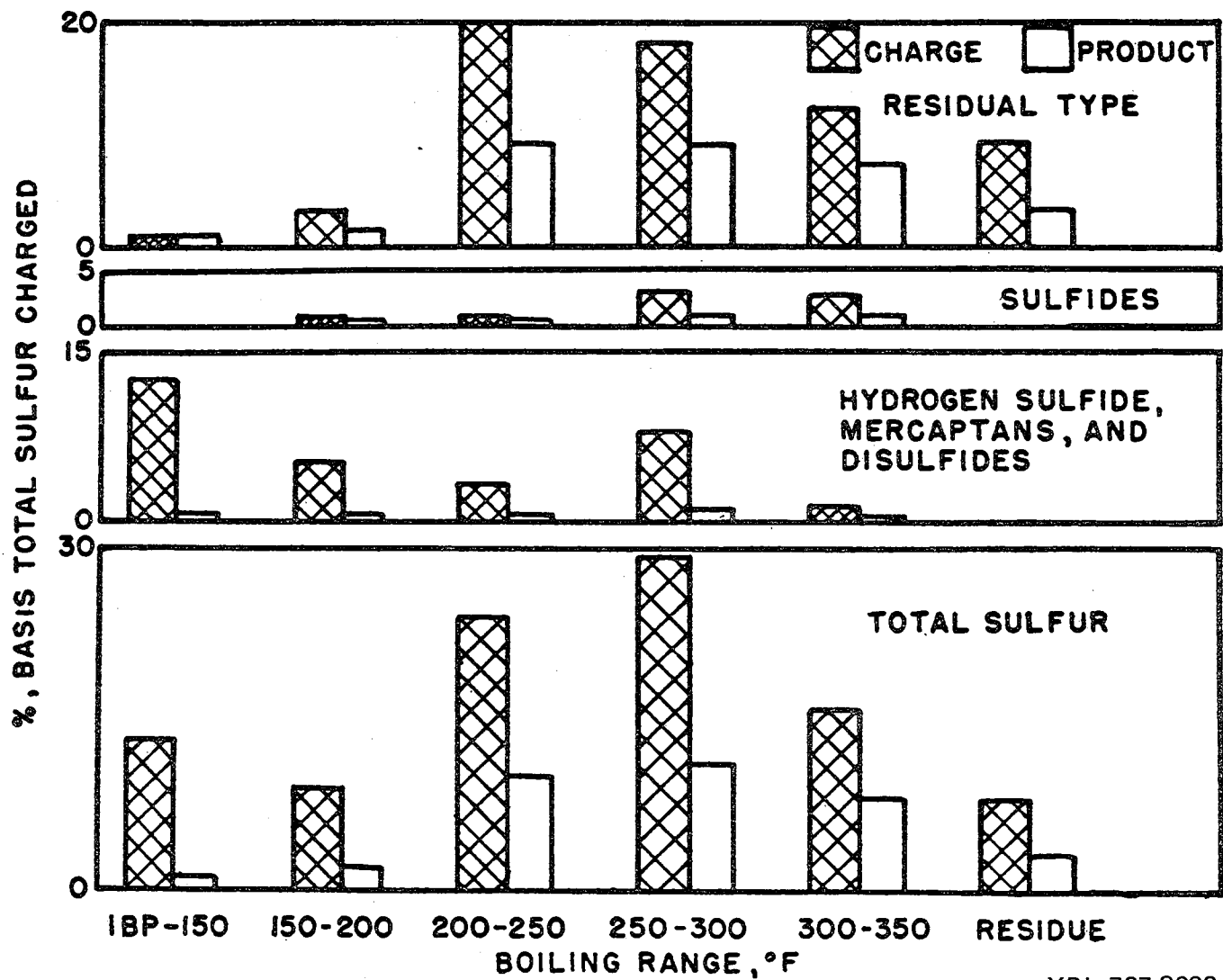
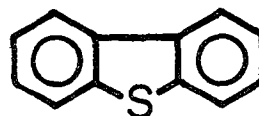


Fig. 2. Sulfur compound distribution in petroleum feedstock

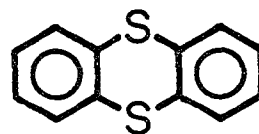
XBL 767-8692

MODEL COMPOUNDS REPRESENTATIVE OF COAL SULFUR SPECIES

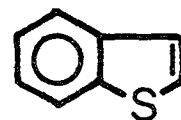
Dibenzothiophene



Thianthrene



Benzothiophene



Diphenyl Sulfide

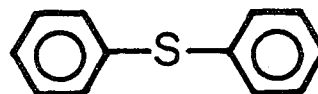


Fig. 3. Model compounds representative of coal sulfur species

XBL795-1514

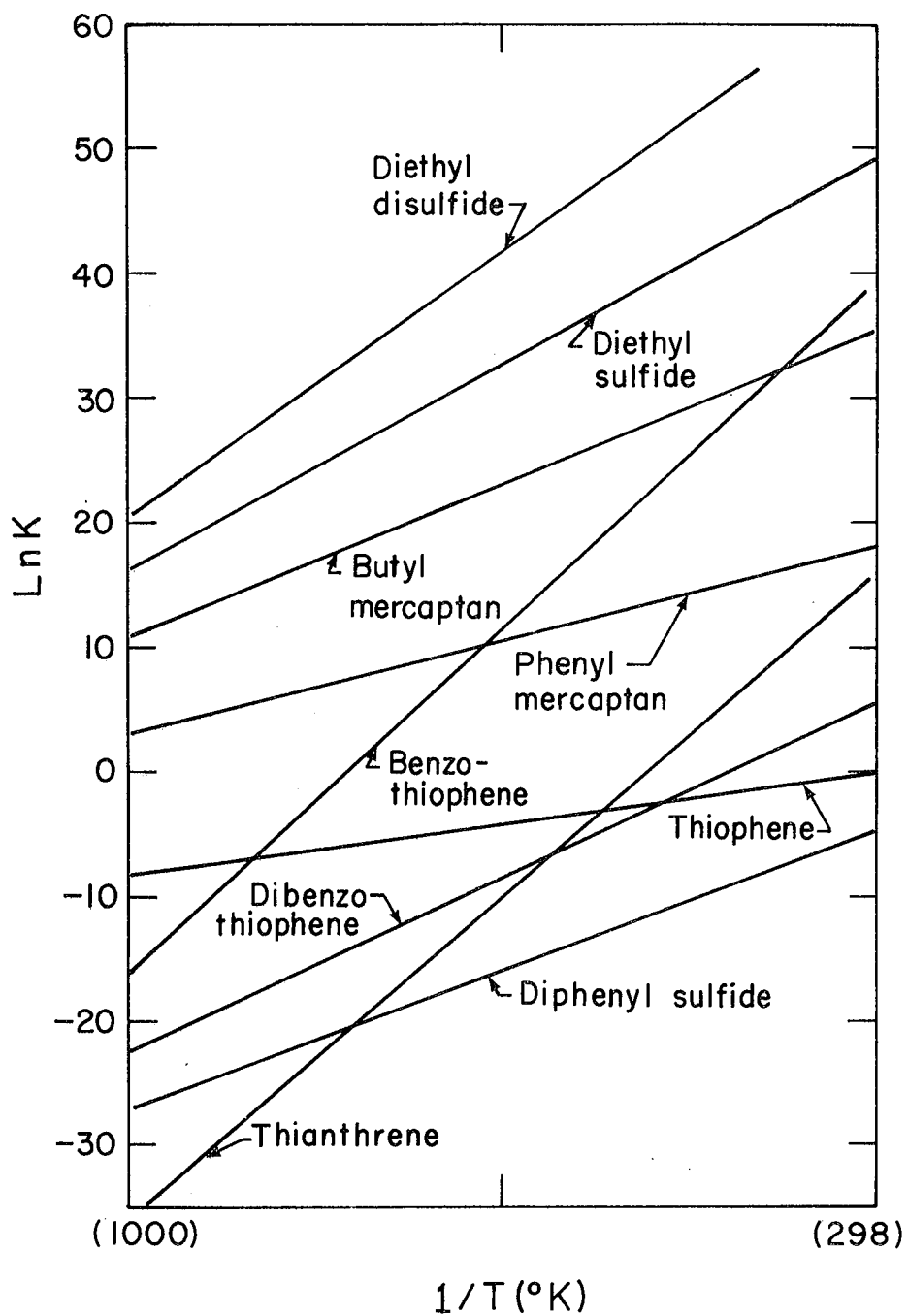


Fig. 4. Hydrodesulfurization thermodynamics of coal sulfur

XBL 795-1509

Table 5 - Physical Coal Cleaning Process Efficiencies

<u>Method</u>	<u>Pyrite Removal</u>
Oil Agglomeration	30-60%
Froth Flotation	50-75%
Gravity Separation	50-75%
Grinding	60-70%
Chemical Comminution	55-70%
Dry Table	60-75%
Magnetic Desulf.	50-80%

From articles in Wheelock, Coal Desulfurization (Ref. 11)

Also known as chemical coal-cleaning, these methods of extraction and leaching rely on the breakage of weaker organic bonds than are found in refractory sulfur compounds, against which they are ineffective (44). Several processes are reviewed in Table 6.

Gas-Solid Reactions:

These reactions involve hydrogenation and pyrolysis, and are usually considered to occur in high-temperature coal conversion processes. H_2S is the principle product of such reactions, and it can be separated and converted to elemental sulfur with existing technology. A number of coal conversion processes are summarized in Table 7. Generalized flow-sheets are given immediately following the table.

Desulfurization During Combustion:

Processes of this sort characteristically involve the use of a bed or an additive to absorb the sulfur in the form of SO_4^{2-} , which then remains with the bed or the ash. This method depends on very inexpensive absorbents, such as soda ash (Na_2CO_3) and limestone ($CaCO_3$).

One process, using fluidized limestone, operates at 1600° F with 3% excess air, minor carbon retention, and 50% efficiency. Regeneration of $CaCO_3$ is claimed after the surface of the limestone becomes sulfated (47).

Another process (McDowell-Wellman Co.) uses pellets of limestone and coal that form little fly ash and trap sulfur in the combusted particle. Unfortunately, no costs or markets for the pellets have been

Table 6 - Description of Chemical Coal Cleaning Processes

Process	Hazen	KVB	Battelle	TRW	Ledgemont	BOM/ERDA
Method	Dry Chemical Pretreatment + Magnetic Sep.	Dry Oxidation + Caustic Wash	Caustic Leach	Acid Leach	Oxygen Leach	Air Leach
Reagent	Fe (CO) ₅	O ₂ , N ₂ , NO, H ₂ O NaOH	NaOH Ca(OH) H ₂ O, CO ₂	Fe ₂ (SO ₄) ₃ H ₂ O, O ₂ Toluene	O ₂ , H ₂ O Lime	AIR, H ₂ O Lime
Pressure (PSIA)	40	35	570	15-80	315	1000
Temp (*F)	383	250	480	162-245	266	392
Retention (Hrs.)	1/2	1	1/4	1/2-10	2	1
Removal Percent, Ash	40	-	-	-	-	-
Pyritic S	100	100	100	100	100	100
Organic S	0	40	25	0	0	40
Sulfur Product	Dry Sulfurous Mineral Matter	Gypsum	H ₂ S Elemental Sulfur	Iron Sulfates Elemental Sulfur	Gypsum	Gypsum

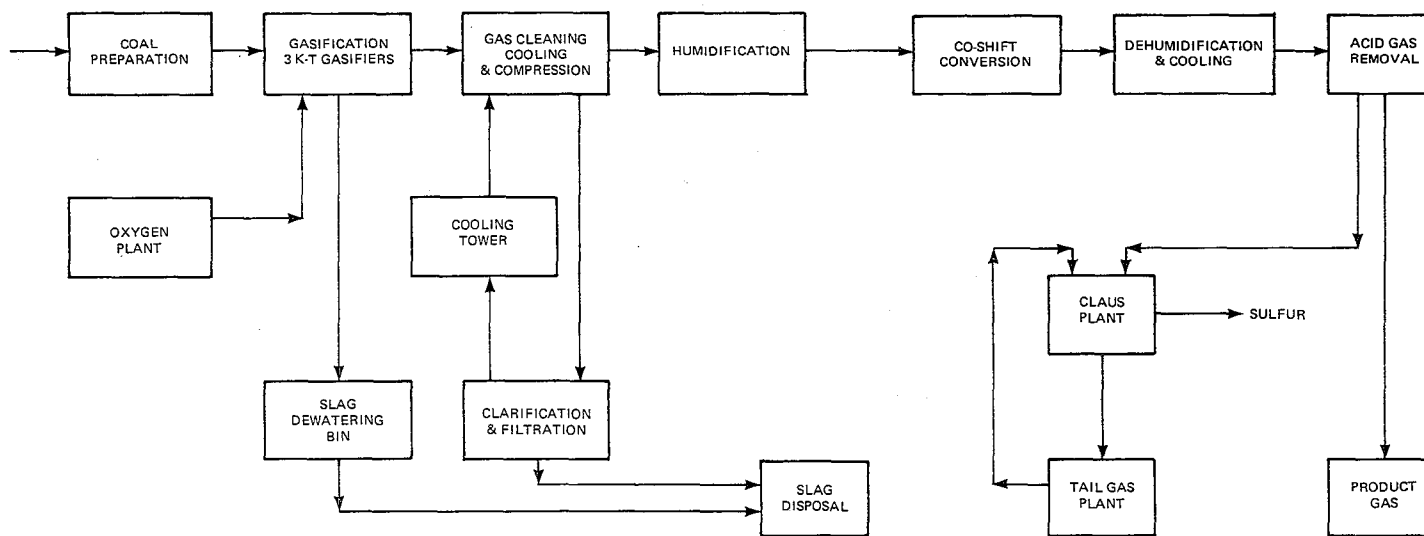
From S. Ergun, Chemical Coal Cleaning Processes (Ref. 44).

Table 7 - Sulfur Removal in Coal Conversion Processes

<u>Gasification Process</u>	<u>Raw Gas %H₂S, COS</u>	<u>BTU/SCF</u>
Lurgi	0.6	302
Winkler	0.29	275
Bi-Gas	0.7	378
Synthane	0.3	405
Hygas	2.9	565
Koppers-Totzek	0.3	298
CO ₂ Acceptor	0.03	440
Molten Salt	0.2	329
U-Gas	0.6	150

<u>Liquefaction Process</u>	<u>Fuel Oil %Sulfur</u>	<u>Liquid Yield</u>
Sasol	0.1	70%
COED	0.1	40%
Toscol	0.2-0.4	50%
Synthoil	0.2	50%
H-Coal	0.16	68%
CSF	0.13	50%
SRC	0.2-0.4	66%

From IGT symposium on Clean Fuels from Coal (Ref. 46).



XBL 795-1507

Figure 5. Simplified flow sheet of a K-T coal gasification complex for producing 100 million std. cu. ft./day of hydrogen. Reproduced by permission of Michaels H. J. and H. F. Leonard, "Hydrogen Production via K-T Gasification" © CEP Aug. 78.

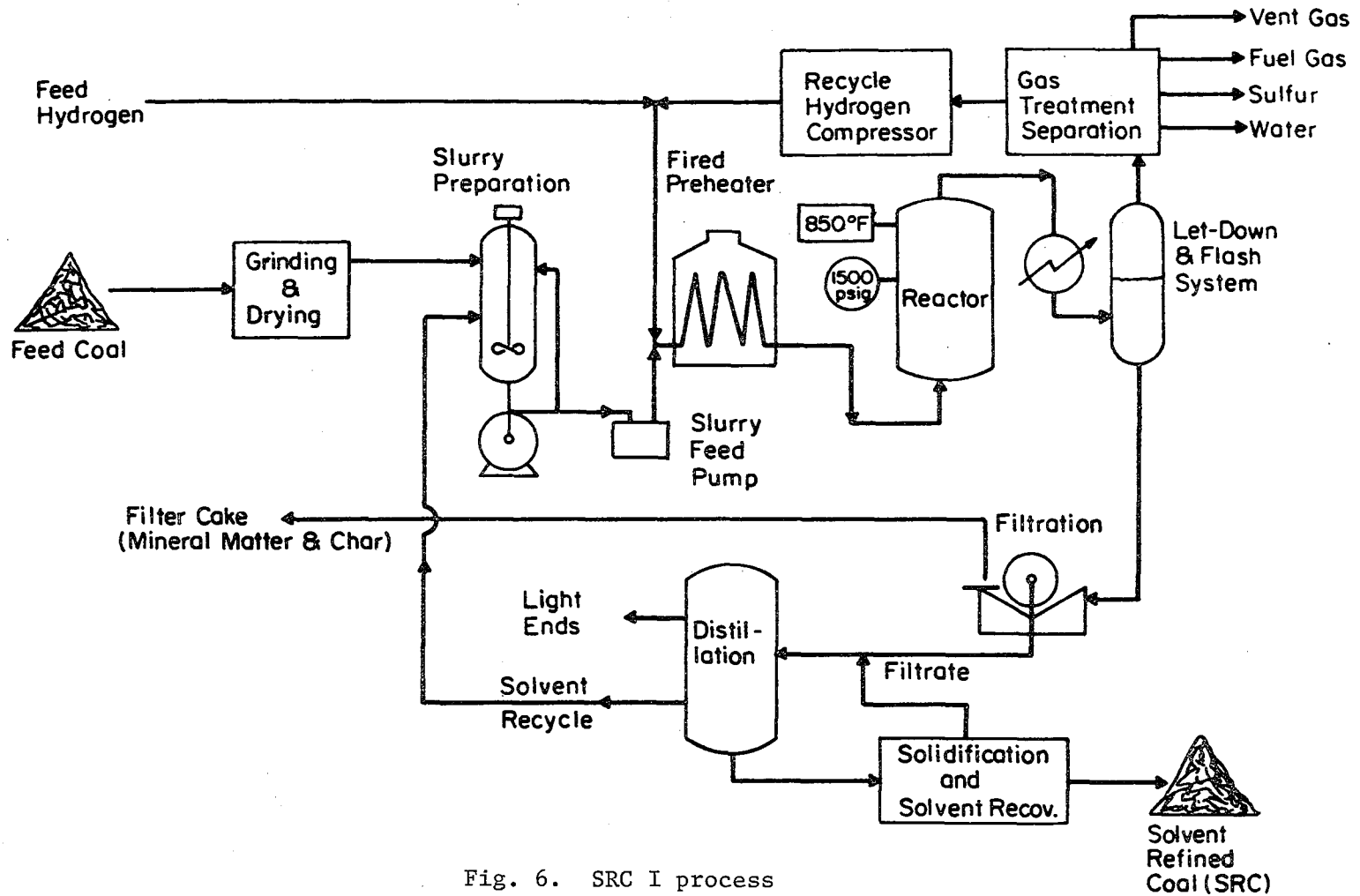


Fig. 6. SRC I process

XBL 767-8691

released, and power plants prefer to use pulverized coal (48).

Desulfurization After Combustion:

This method, flue-gas scrubbing, amounts to the existing desulfurization technology, along with physical methods. Unfortunately, flue-gas operations are normally either expensive or unreliable or both. A summary of some flue-gas processes is given in Table 8.

E. Applicability of Cleaning Processes to U. S. Coals

Since current coal cleaning processes remove only a fraction of the total sulfur (50), the question arises as to what fraction of U. S. coals can be cleaned within current E.P.A. new source standards (1.2 lb. SO₂ per MMBTU). A number of studies has shown the fraction to be encouragingly large.

A report on the applicability of the Meyers process (51) estimates, on the basis of 35 coals sampled, that 40% of the samples could be burned cleanly after some combination of physical separation and chemical leaching (see Fig. 7).

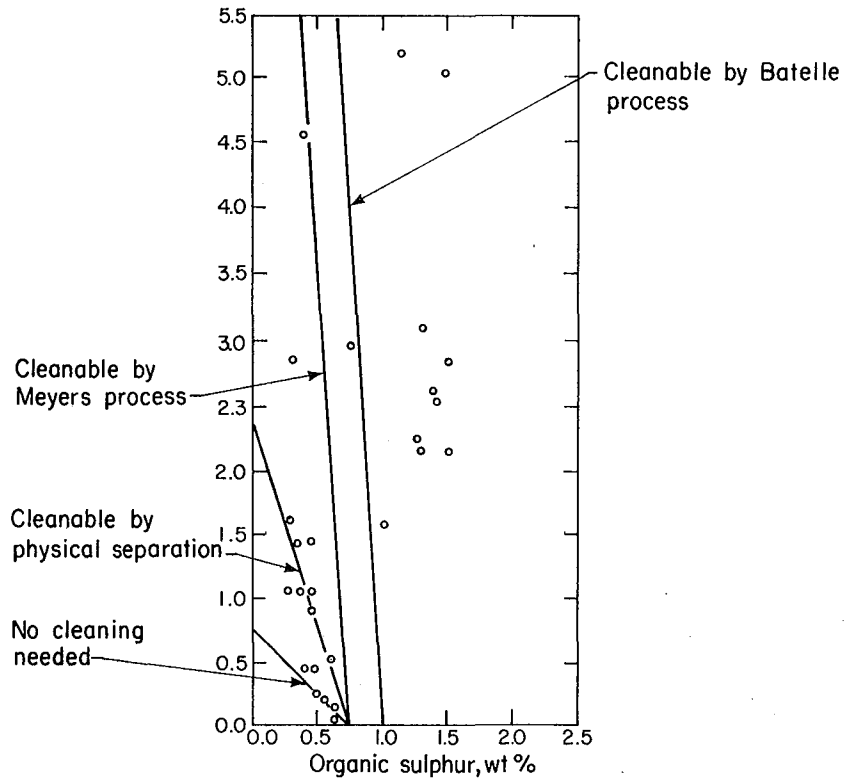
A report by Sabri Ergun (52) on coal cleaning gives the higher estimate of cleanability of 56%, based on 455 samples properly weighted between Eastern and Western coals. Beyond this figure, Ergun estimates an additional 17% is cleanable if 30-40% of the organic sulfur is removed, bringing the total cleanable to 73%.

Data from a study by Cavallaro (53), with coal reserves taken from a study by Beekers (54), give an estimate in agreement with that of

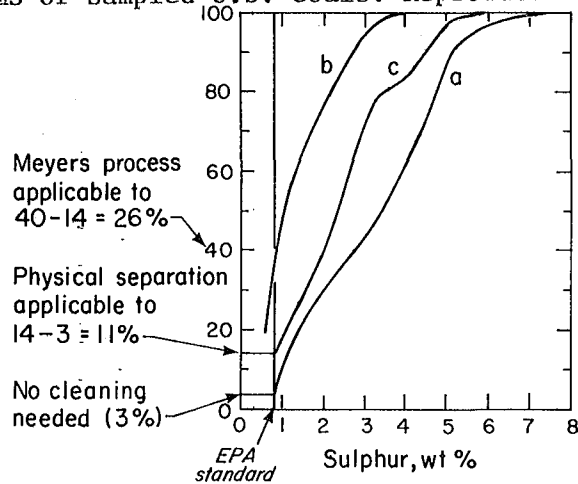
Table 8 - Technically Feasible Flue-Gas Operations

<u>System</u>	<u>Reactions</u>	<u>Reliability</u>
Lime-Limestone	$\text{SO}_2 + \text{CaO} \rightarrow \text{CaSO}_3$ $\text{CaCO}_3 + \text{Heat} \rightarrow \text{CaO} + \text{CO}_2$ $\text{CaSO}_3 + \frac{1}{2}\text{O}_2 \rightarrow \text{CaSO}_4(\text{s})$	Poor
Double Alkali	$\text{SO}_2 + \text{Na}_2\text{SO}_3 + \text{H}_2\text{O} \rightarrow 2\text{NaHSO}_3$ $2\text{NaHSO}_3 + \text{Ca}(\text{OH})_2 \rightarrow$ $\text{CaSO}_3(\text{s}) + \text{Na}_2\text{SO}_3 + 2\text{H}_2\text{O}$	Fair
Chiyoda	$\text{SO}_2 + \text{H}_2\text{O} + \text{H}_2\text{SO}_4 \rightarrow 2\text{H}_2\text{SO}_3$ $2\text{H}_2\text{SO}_3 + \text{O}_2 \rightarrow 2\text{H}_2\text{SO}_4$ $\text{H}_2\text{SO}_4 + \text{CaCO}_3 \rightarrow \text{CaSO}_4(\text{s}) + \text{H}_2\text{O}$ $+ \text{CO}_2$	Good
Magnesium Oxide	$\text{MgO} + \text{SO}_2 \rightarrow \text{MgSO}_3(\text{s})$ $\text{MgSO}_3 + \text{Heat} \rightarrow \text{MgO} + \text{SO}_2$ $\text{SO}_2(\text{Conc.}) + \text{H}_2\text{O} + \frac{1}{2}\text{O}_2 \rightarrow \text{H}_2\text{SO}_4$	Good
Wellman-Lord	$\text{Na}_2\text{SO}_3 + \text{SO}_2 + \text{H}_2\text{O} \rightarrow 2\text{NaHSO}_3$ $2\text{NaHSO}_3 + \text{Heat} \rightarrow \text{Na}_2\text{SO}_3 + \text{SO}_2$ $+ \text{H}_2\text{O}$ $\text{SO}_2(\text{Conc.}) + \text{H}_2\text{O} + \frac{1}{2}\text{O}_2 \rightarrow \text{H}_2\text{SO}_4$	Good

From Herlihy, Flue Gas Desulfurization in Power Plants (Ref. 49).



Sulfur forms of sampled U.S. coals. Reproduced by permission of ACS, C 1977.



Sulfur content of survey run-of-mine coals (curve a) the same coals physically cleaned (curve c) and chemically desulfurized (curve b) Reproduced by permission of ACS, C 1977 XBL 795-1511

Fig. 7. U. S. Coal Cleanability

Ergun on the amount of coal cleanable by pyrite removal. The data are presented in Table 9.

In summary, it can be seen that cleanable coal reserves increase by 33% if processes are used which can remove what are probably the more reactive organic sulfur species (55), such as aliphatic mercaptans, sulfides, and disulfides. A process which attacks the refractory thiophenic sulfur could conceivably increase the cleanable coal reserves by another 20 - 30%, assuming roughly equal distribution between reactive and refractory organic sulfur. The basis for this study is to find such a process and, if possible, determine its economic feasibility.

F. Objectives of This Study

An inexpensive method of pre-treating coal to remove refractory organic sulfur is clearly desirable. At present, no such process exists. Best existing technology, as was shown earlier, can only attack the relatively reactive aliphatic sulfides, disulfides, and mercaptans, which do not account for the total organic sulfur content of most coals. An examination of the chemistry of refractory sulfur species may point to a reagent suitable for treatment of coal and/or coal-derived materials.

G. Chemistry of Model Compounds

Previous extractive studies have isolated typical refractory sulfur compounds in coal (36,39). Some work towards desulfurization has been

Table 9 - Coal Reserve Cleanability, B.O.M. Data*

Coal	MMBTU/ton,ROM	10 ⁶ ton res.	Quad res.	% clean, ROM + % cleanable
Northern Appalachian	22.34	72920	1629	12
Southern Appalachian	23.43	37349	875	50
Alabaman	24.10	2982	72	35
Eastern Midwest	21.45	88912	1907	2
Western Midwest	21.25	15720	334	4
Western	18.66	216065	4032	94
Total (Average)	(20.39)	433948	8849	(51)

1979 U. S. Coal Consumption (estimated) 14.89 quads.

1979 U. S. Energy Consumption (estimated) 68 quads.

*Based on proposed E.P.A., new source standards of 1.2 lb. SO₂/MMBTU.

done on all these compounds. It is assumed that thiophene is strictly an artifact of pyrolysis or other severe processes, and that it only occurs as a highly substituted molecule in the coal matrix. Attempts at desulfurization are summarized in Table 5 (56). Only cobalt-molybdenum-alumina is consistently useful of the many techniques studied in model-compound desulfurization (52).

Strong reducing agents are particularly useful in conversion of refractory organic sulfur species to desulfurized forms (58). One relatively inexpensive agent that has been studied to some extent is metallic sodium, either alone, in combination with NH_3 , or in amalgam form.

H. Chemistry of Sodium

Sodium is a standard reagent in numerous organic reactions, some of which are listed in Table 11 (59). Of more interest to fuel chemists is the use of sodium in the desulfurization of a wide range of hydrocarbon feedstocks (59,60), both experimentally and commercially. Included in the list of compounds for which sodium desulfurization has been attempted are naphthalene (59), benzene, gasoline (60), various petroleum fractions (59,61,62), lubricating oil (65), and petroleum residua (64).

Another property of sodium of interest to fuel chemists is its hydrogenating and ether cleavage activity. In combination with

Table 10 - Methods Studied for Desulfurization of Model Compounds

	Diphenyl- sulfide	Benzo- thiophene	Dibenzo- thiophene	Thianthrene
AlCl ₃	X	X	X	
ZnCl ₂	X		X	
MoS ₂		X	X	
CoMo		X		
MoO ₃ - CoO- Al ₂ O ₃		X	X	
Raney Nickel		X	X	
NaRb			X	
H ₂ SO ₄		X	X	
NH ₄ -Y- Zeolite			X	
KOH			X	
Pyrol.			X	X
Na	X	X	X	X

Table 11 - Organic Reactions of Sodium

Comparison of Lithium and Sodium in Organic Reactions

Reaction	Product	Yield Obtained	
		With Lithium	With Sodium
Ether formation with alkoxide	$C_6H_5CH_2OC_2H_5$	63.0	77.0
Fittig synthesis	$C_6H_5C_2H_5$	39.5	51.8
Acid salt plus acid chloride	$(CH_3CO)_2O$	53.0	56.0
Alkylation	$CH_3COCH(C_2H_5)CO_2C_2H_5$	72.0	62.0
	$C_2H_5CH(CO_2C_2H_5)_2$	72.0	70.0
Condensation with alkoxide	$CH_3COCH_2CO_2C_2H_5$	1.4	11.0
	$CH_3COCH_2COCO_2C_2H_5$	18.6	34.9
Perkin synthesis	$C_6H_5CH:CHCO_2H$	9.0	47.0
Pinacol synthesis	Pinacol	6.9	7.1
Orthoformate synthesis	$HC_5(OC_2H_5)_3$	5.0	22.0
Ketone from acid salts by dry	$(CH_4)_2CO$	93.0	50.0
Distillation	$(C_6H_5)_2CO$	50.0	28.2

From Sittig, Sodium (Ref. 59).

R-NH₂ (59) or R-OH (59,65), sodium will hydrogenate aromatic and unsaturated aliphatic compounds. In a solution of NH₃, sodium will cleave ethers and aid in hydrogen transfer to the cleaved species (66,67). It is believed that ether cleavage of medium-boiling hydrocarbons by sodium is the predominant reaction in a process known as gasoline degumming (59).

A number of studies have been reported on the desulfurization of model compounds with sodium. Benzothiophene is the chief sulfur impurity in both gasoline and naphthalene (59,60). Dibenzothiophene has been studied by Sternberg with good results (64). Finally, Clegg studied the desulfurization of mercaptans, sulfides, disulfides, and thiophene using sodium (68). Because these model compounds have either been identified in or associated with coal, sodium is seen as a promising agent in coal-liquid desulfurization, assuming that competing reactions don't exhaust the sodium prior to desulfurization activity. Reactions of sodium are summarized in Figure 8.

HYDROGENATION REACTIONS WITH SODIUM

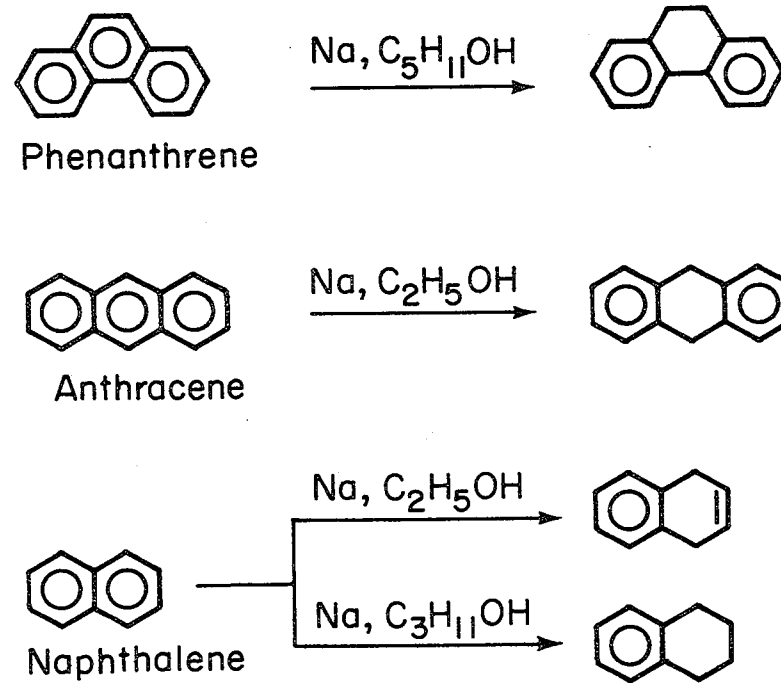


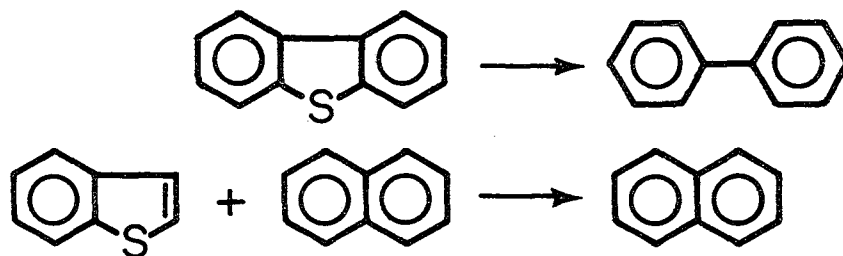
Fig. 8. Desulfurization and hydrogenation reactions of sodium

XBL 795-1621

DESULFURIZATION REACTIONS WITH SODIUM

Heavy Petroleum Fractions → 50% Desulfurization

Gasoline → 99% Desulfurization



XBL 795-1512

Fig. 8 (cont.)

II. EXPERIMENTAL

A. Apparatus

1. A three-necked 500 or 1000 ml flask was used as the reaction vessel for runs at atmospheric pressure. The flask was fitted with condenser, N₂ feed, thermometer or thermocouple, and mercury-seal stirring rod holder. The reaction temperature was maintained at 200° C by varying the power to a heating mantle using a Variac.

The same flask was used for vacuum distillation. It was fitted with a vacuum gauge, a heated Claisen condenser, and an iron-constantan thermocouple. Distillate was collected in an ice-cold filter flask. House vacuum (-27 in. Hg) was used.

2. For high-pressure runs, a Hastelloy Parr bomb was used. Temperature was monitored with an iron-constantan thermocouple and strip-chart recorder, and was controlled with an 800-watt heating mantle and cooling coil. The bomb was stirred at 600 rpm. Samples were removed at appropriate times through the sample tube into a heat exchanger wherein they were cooled and collected into filter test tubes. In some cases, a standard U. S. Steel Chemists H₂S absorber (69) of four to six stages was attached to the vent valve of the bomb. Pressure was regulated at 5 psig in the absorber and flow rate was adjusted to avoid bubbling into the tubing connecting the stages.

Table 12 - Experimental Chemicals

1. Desulfurization of model compounds:

Biphenyl	Eastman-Kodak	Technical	721
Decahydronaphthalene	Aldrich	Technical	D25-1
Dibenzothiophene	Aldrich	95%	D3,220-2
Diphenyl Sulfide	Eastman-Kodak	Technical	619
Ehtyl Benzene	Matheson, Coleman, & Bell	Technical	5026
Sodium Dispersion	Matheson, Coleman, & Bell	40% Na, 60% Oil	SX233
Thianaphthene	Eastman-Kodak	97%	T2,740-5
Thianthrene	Aldrich	Technical	3315

2. H₂S Absorption:

CdCl ₂ *2½H ₂ O	Mallinckrodt	Analytical	4000
Na ₂ S*9H ₂ O	Baker	100.7%	8036
NH ₄ OH	Mallinckrodt	27%	3248

3. Sludge Fixation

BaCl ₂ *2H ₂ O	Mallinckrodt	Analytical	3756
CaO	Mallinckrodt	Analytical	4243
Na ₂ SO ₄	Mallinckrodt	Anhydrous	8016

4. Miscellaneous:

HCl	Mallinckrodt	37%	2612
-----	--------------	-----	------

B. Chemicals

A list of chemicals, with manufacturer, grade or purity, and stock number, is given in Table 12.

In addition to the chemicals listed in Table 12, three kinds of coal-related materials were used, analyses of which appear in Table 13. Solid solvent-refined coal (SRC) was produced in a pilot plant at Fort Lewis, Washington, operated by Pittsburgh and Midway Mining Co. Stripper bottoms recycle slurry was obtained from the SRC pilot plant operated by Catalytic, Inc., at Wilsonville, Alabama. Illinois #6 coal was provided by the Illinois Geological Survey and was prepared as described by Mendizabal (70).

Table 13 - Ultimate Analyses of Coal-related Materials

<u>Material</u>	<u>Solid SRC</u>	<u>Recycle Slurry</u>	<u>Illinois #6</u>
% Carbon	84.82	82.57	54.97
% Hydrogen	4.89	6.29	4.54
% Nitrogen	2.56	1.30	0.92
% Sulfur	0.69	0.99	3.54
% Ash	0.50	3.80	16.0

A typical SRC flow diagram (71) is given in Figure 6.

The streams from which recycle slurry and solid product derive are labeled on the flow diagram.

In the case of solid SRC, a comparison of dry analyses yields the following distribution:

Table 14 - Feed Coal and Product SRC Composition

<u>Feed Coal</u>		<u>Solid SRC</u>			
%C	64.30	moles C	1.00	84.52	1.00
H	4.47	H	0.834	4.89	0.692
O	9.07	O	0.106	6.54	0.0578
N	1.33	N	0.0177	2.56	0.0259
S	4.00	S	0.0233	0.69 (TOTAL)	0.00305
S _p	2.4	S _p	0.0140	- (DYRITIC)	-
S _a	0.8	S _a	0.00467	- (ALIPHATIC)	-
S _t	0.8	S _t	0.00467	0.69 (THIOPHENIC)	0.00305

The discrepancy in molar ratios of S_t/C between feed and solid product probably results from an even higher S_t/C ratio in the heavy mineral residue slurry that is a co-product of the solid process.

C. Analyses

1. Gas Chromatography:

Gas Chromatograph analyses of model compounds were made in a Chromalytics gas chromatograph, using an 8% dexsil column on Chromo G HP packing (80/100 mesh). The temperature programmer was set at 60-100° C initially, and run to 340° C at a rate of 12-20° C per

minute. Helium was the carrier gas. Detection of peaks was done with flame ionization and thermal conductivity detectors. The solvent (decalin) peak height and impurity (model compound) peak height were measured, and calibration curves of molar concentration vs. relative peak height were prepared. These curves were used to plot concentration vs. time for the various model compound runs.

2. Sulfur Analysis:

Solids and slurries were analyzed using a furnace at 850° C, Oxygen flow at 10 ml/min. and atmospheric pressure, residence time of 15 min., and sample size of 10-50 mg. The resultant SO₂ was oxidized to H₂SO₄ by H₂O₂, and precipitated with acidic BaCl₂. The resulting BaSO₄ was filtered, dried, and weighed. In cases where sulfur remained in the residue, the residue was washed in acidic BaCl₂ as above.

3. Carbon-Hydrogen-Nitrogen:

These analyses were made using a Perkin-Elmer 240 C-H-N analyzer. Combustion occurred at 950° C in a large excess of oxygen. H₂O, CO₂, and N₂ produced were measured by a thermal conductivity detector.

A large excess of WO₃+V₂O₅ is added to samples containing alkali metals or earths.

4. Sodium and other metals:

Samples with sodium present were digested in H₂SO₄, from which solutions were prepared. The atomic absorption spectra were then

obtained and compared with a curve of known standards.

5. Number-average Molecular Weight:

Molecular weight determinations were performed on a 302B Hewlett-Packard Vapor-pressure osmometer. Concentration series were prepared, and a 100 uV recorder was used to record temperature changes for the series. The resulting vapor pressure vs. concentration curves were plotted to yield $(V/C)_0$.

The number-average molecular weights were calculated relative to K-factors for reserpine, MW 608, the reference compound.

SRC materials were chosen because it is suspected that their organic sulfur content is entirely thiophenic. This means that the hydrogenation step in the SRC process converts pyrite (FeS_2) into pyrrhotite (FeS) (70) and aliphatic sulfur species into alkane groups. As was seen in Fig. 4, the hydrodesulfurization of thiophenics is not favorable at SRC reaction conditions (1500-2000 psig H_2 , 470 °C), so the sulfur leaving the stripper following the reactor is entirely thiophenic or pyrrhotitic.

In the case of slurry recycle, the feed coal is 4% sulfur and the recycle solvent is 0.2% sulfur, with a coal-to-solvent ratio of 2:1. The feed sulfur is 60% pyritic, and the remainder is assumed to be equally distributed between aliphatic and thiophenic. Using these data and the mass flows shown in Fig. 24, the mass balance shown in Fig. 9 results. The estimated sulfur content of 0.87% compares favorably

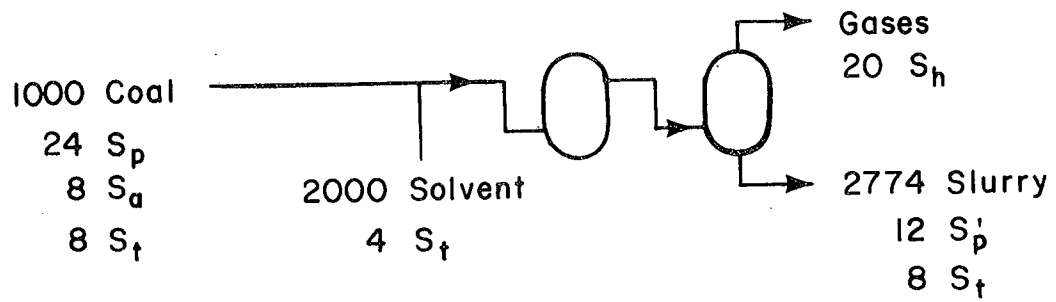


Fig. 9. Mass balance for SRC sulfur distribution

XBL 795-1508

- S_p = Pyritic sulfur
- S_a = Aliphatic sulfur
- S_t = Thiophenic sulfur
- S_p' = Pyrrhotitic sulfur
- S_h = H₂S sulfur

with the actual content of 0.99%, implying slightly less complete hydrodesulfurization of pyrite and aliphatic sulfur than was assumed.

III. RESULTS AND DISCUSSION

A. Model Compounds

First experiments were concerned with finding the appropriate ratio of sodium to sulfur to insure fairly complete conversion for the reaction:



where DBT = dibenzothiophene and BP = biphenyl. Given the conditions of 24 hours reaction time, 200 ° C, atmospheric N₂ pressure, results are shown in Figure 10. These results agree with a previous author (72), who found that a 3/1 molar ratio of sodium to sulfur was required.

The next experiment was conducted in order to determine the time required for reaction. The same conditions of temperature and pressure were used. Graph 11 shows that good conversion was obtained after one to two hours of reaction.

Similar experiments were conducted with thianaphthene, diphenyl sulfide, and thianthrene to determine the effect of sodium on conversion to desulfurized products. Conditions of reaction were 50 psig each of N₂ and H₂ at 200° C. In these runs there was a heat-up time of 15 minutes, during which time little reaction occurred. Results are shown in Graphs 12, 13, and 14.

In each case, the desulfurized product yield is much lower than expected from degree of conversion. Two possibilities suggest them-

EFFECT OF MOLAR RATIO ON CONVERSION OF DIBENZOTHIOPHENE

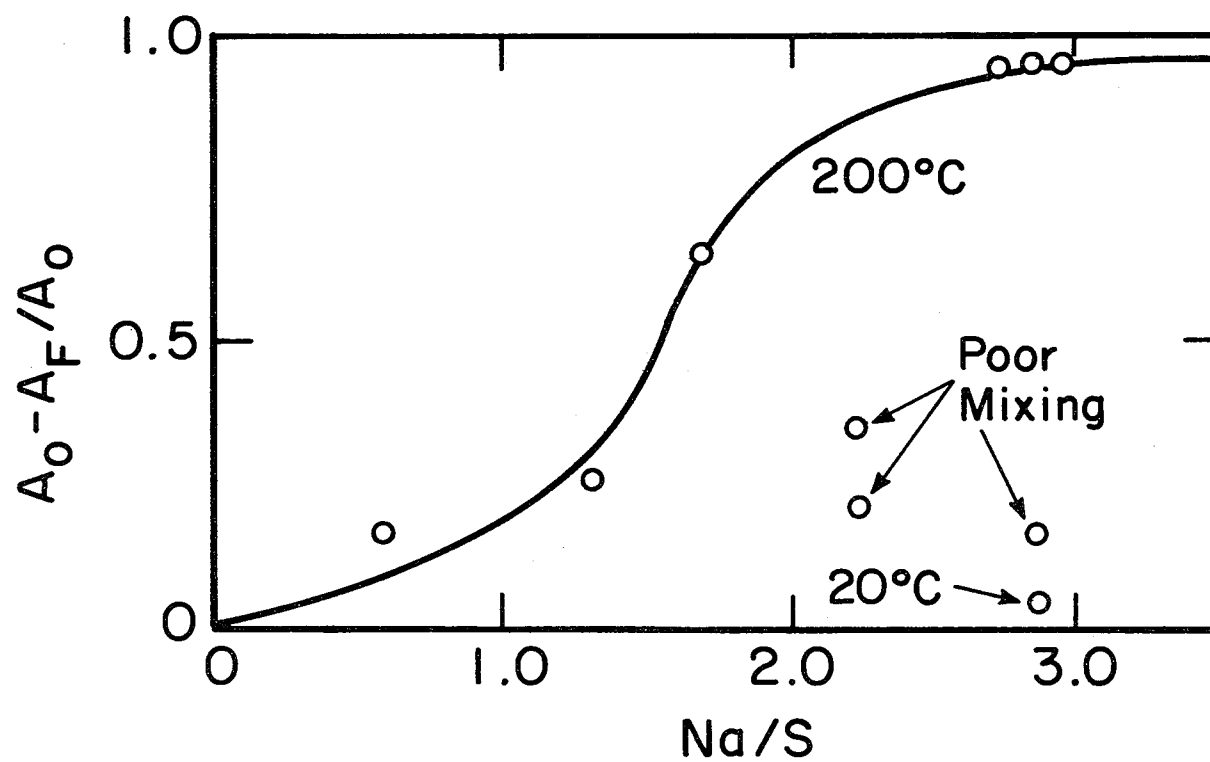


Fig. 10. Dibenzothiophene desulfurization vs. molar Na/S

DESULFURIZATION OF DIBENZOTHIOPHENE (DBT) TO BIPHENYL (BP)

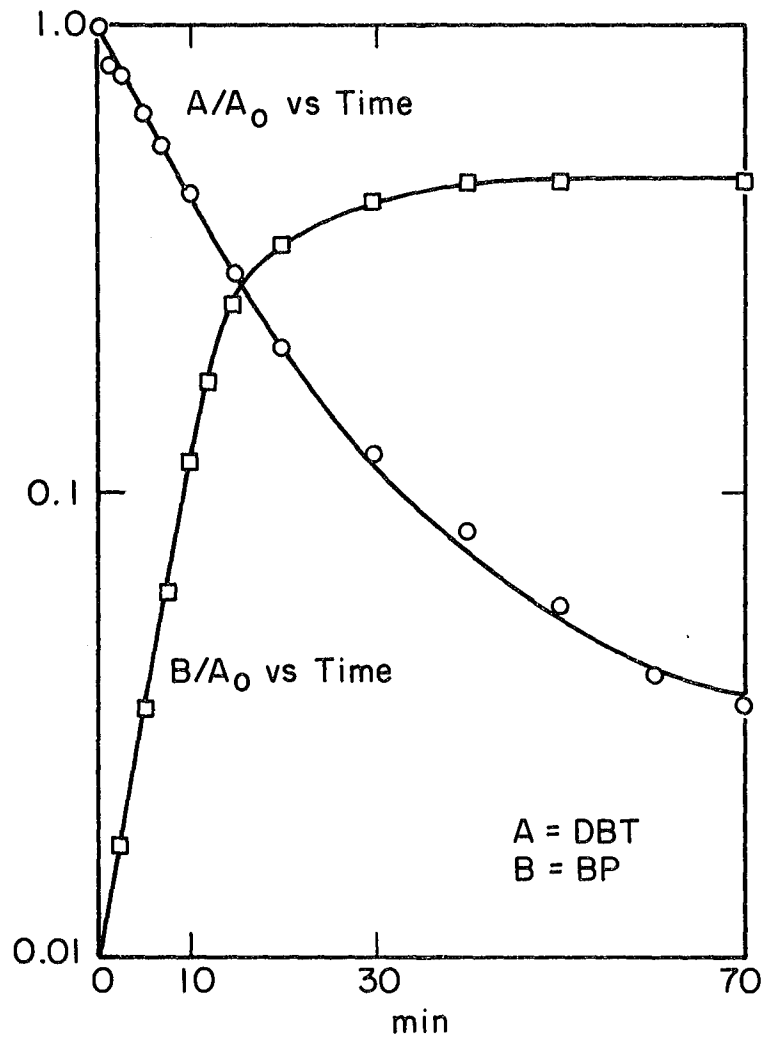
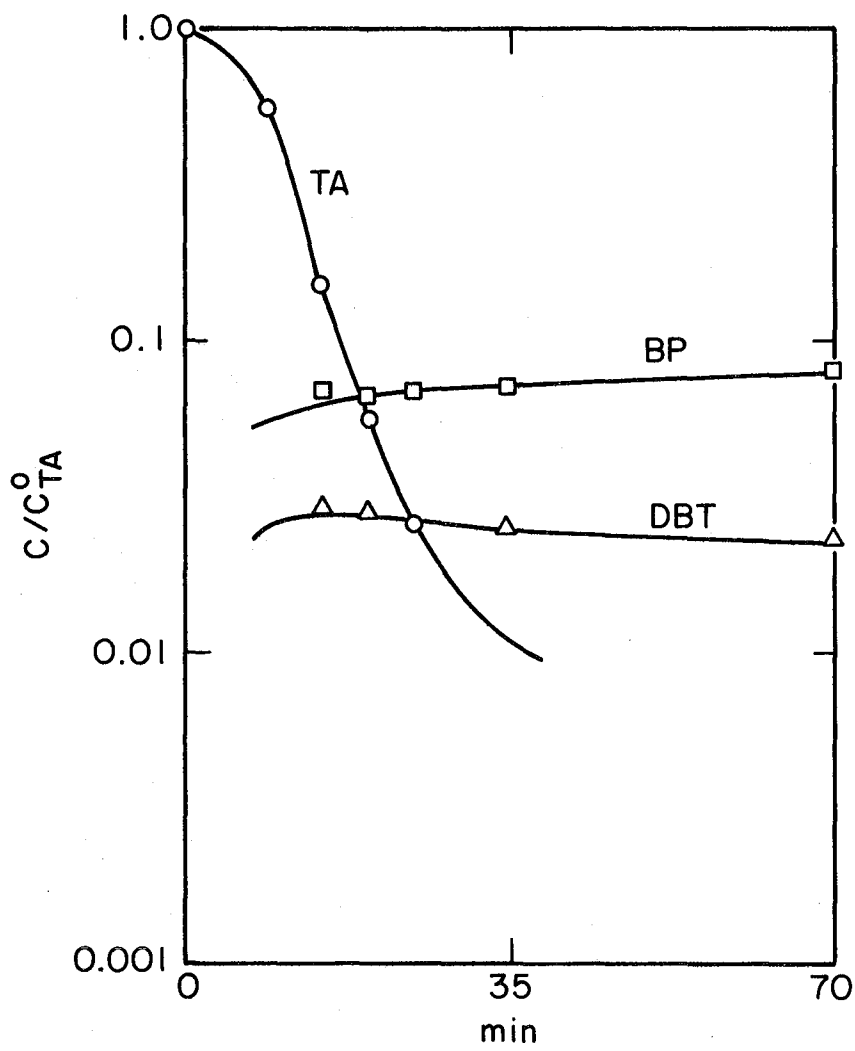


Fig. 11. Dibenzothiophene desulfurization vs. time

XBL 795-1515

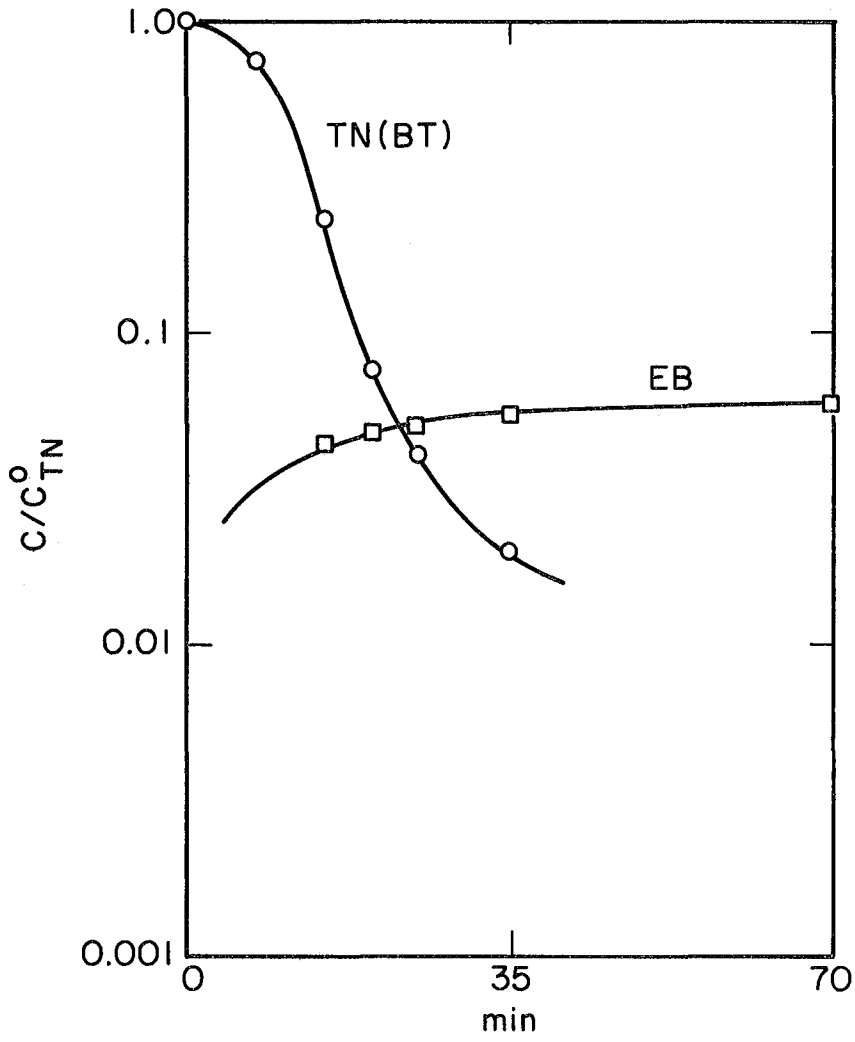
DESULFURIZATION OF THIANTHRENE (TA) TO DIBENZOTHIOPHENE (DBT)
AND BIPHENYL (BP)



XBL795-1516

Fig. 12. Thianthrene desulfurization vs. time

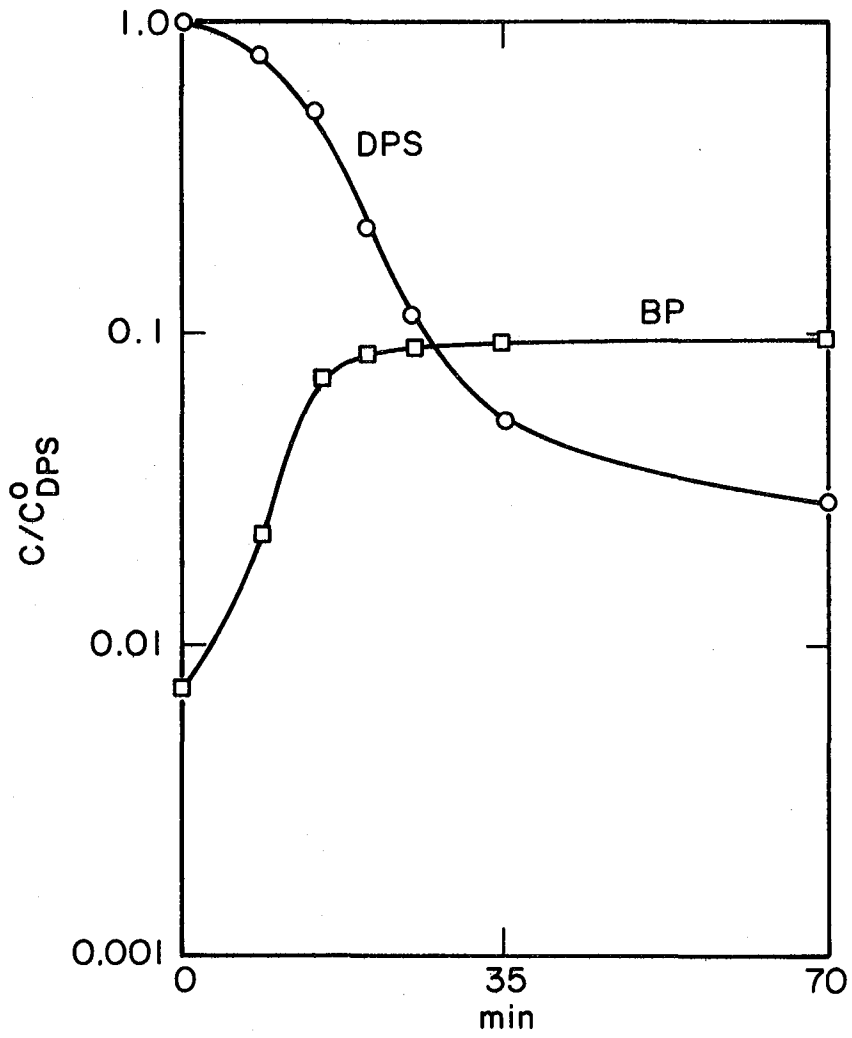
DESULFURIZATION OF BENZOTHIOPHENE (BT) TO ETHYL BENZENE (EB)



XBL 795-1517

Fig. 13. Benzothiophene desulfurization vs. time

DESULFURIZATION OF DIPHENYL SULFIDE (DPS) TO BIPHENYL (BP)



XBL 795-1518

Fig. 14. Diphenyl sulfide desulfurization vs. time

selves. The first is that highly volatile products such as benzene were formed, thus escaping detection by the G.C. It can be seen that benzene results from cleavage of thianthrene and diphenyl sulfide if hydrogen is available to cap off the radicals involved.

In the case of benzothiophene, styrene is the immediate product of desulfurization. This product can then form ethyl benzene, or polymerize to form a distribution of soluble polymer species which would also escape detection by the G.C.

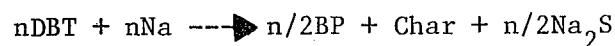
Finally, char from the 400 psig H₂ and N₂ runs was analyzed in pyridine using the vapor pressure osmometer. Standard solutions of 7.33 and 7.06 g/kg, respectively, were diluted to 3/4, 1/2, 1/4, and 1/8 of C_o, and the voltage change for each due to heat of condensation was recorded. The standard curve for reserpine, MW 608, was prepared (73) and from this a standard K-value was calculated:

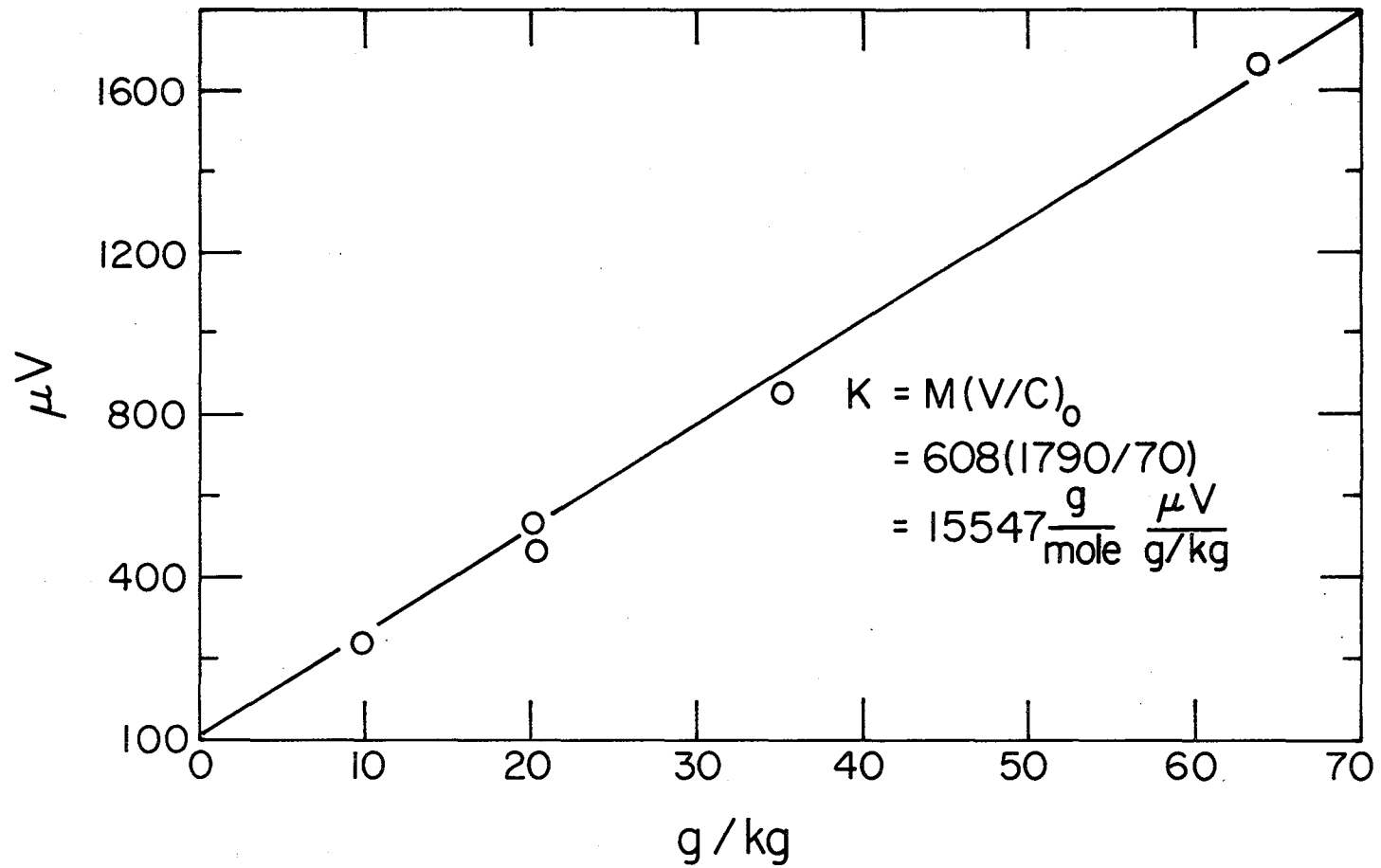
$$K = MW(V/C)_o = 15547 \text{ (g/mole) (uV/g/kg)}$$

Since (V/C)_o for the H₂-char was 9.754 uV/g/kg, the number-average molecular weight for this char was 15547/9.754, or 1594. Similarly, the molecular weight of the N₂ char was 15547/7.649, or 2033. Results are shown in Graphs 15, 16, and 17.

B. Mechanism of Dibenzothiophene Desulfurization

The overall reaction of dibenzothiophene (DBT) and sodium is as follows:

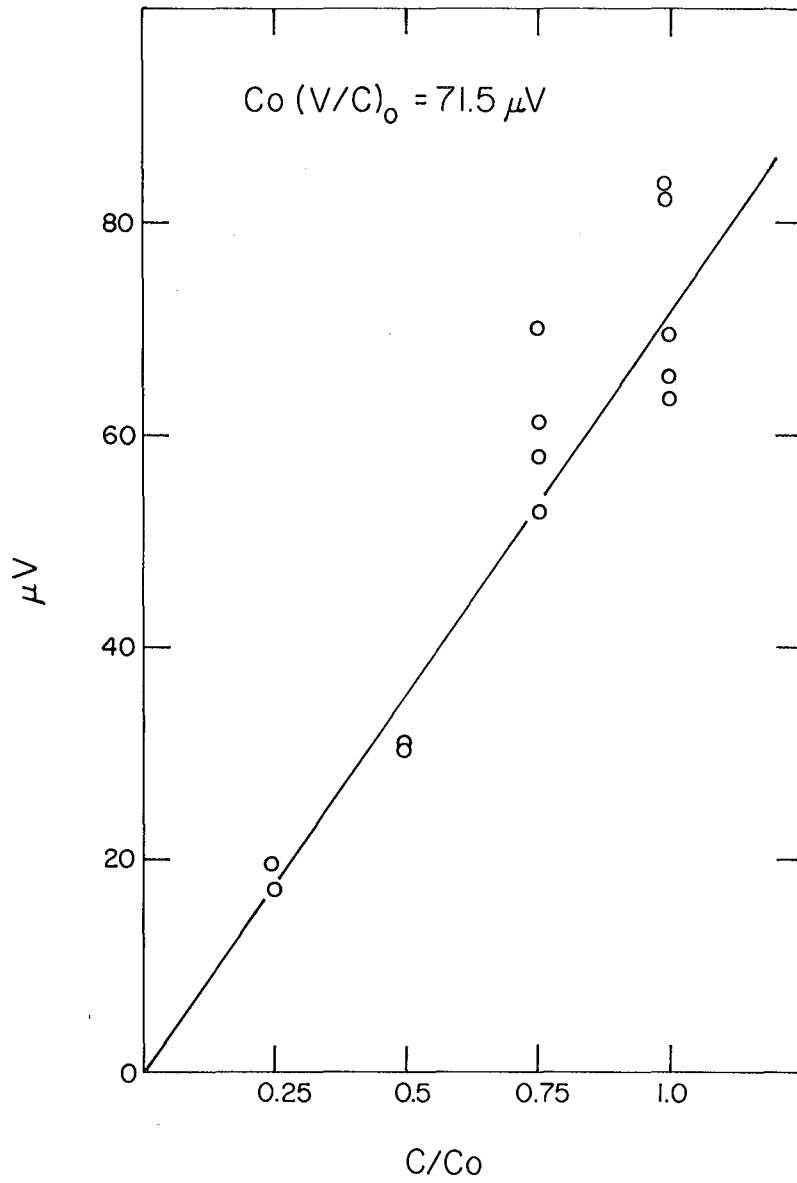




-47-

Fig. 15. Reserpine K-curve desulfurization vs. time

XBL 795-1506



XBL 795-1505

Fig. 16. Hydrogen-char VPO curve

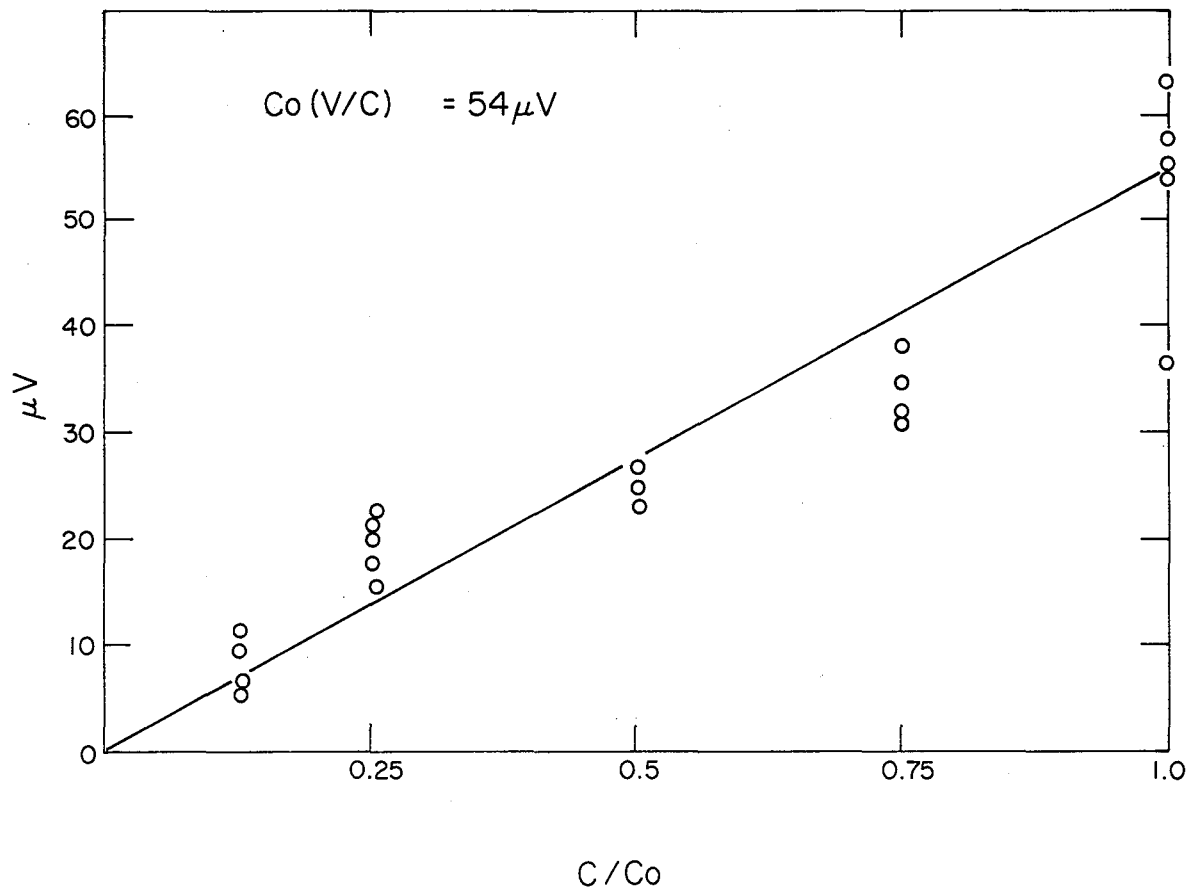


Fig. 17. Nitrogen-char VPO curve

XBL 795-1504

The desulfurized product is biphenyl (BP). Sternberg proposed the following mechanism, illustrated in Figure 18, based on the analogous reaction between lithium and DBT proposed by earlier workers.

The initial reaction is formation of a radical anion, which then proceeds through several steps to form a species similar to BP. This species then either polymerizes to form char or exchanges its Na for H to form BP. To explain the effect of H_2 in inhibition of the overall reaction, Sternberg suggests that NaH formation occurs, and that the NaH is less active than Na in formation of radical anions.

Our results on the kinetics of the reaction between sodium dispersion and DBT are shown in Figure 11. The run was conducted under atmospheric N_2 at $200^\circ C$ with a molar ratio of $Na/DBT = 3$, and samples were taken at intervals throughout the run.

Numerous mechanisms were devised and rate expressions were derived and solved in terms of $f(A/A_0) = kt$, where A represents DBT. It was found that the following expression fitted the experimental curve with least deviation in the value of k:

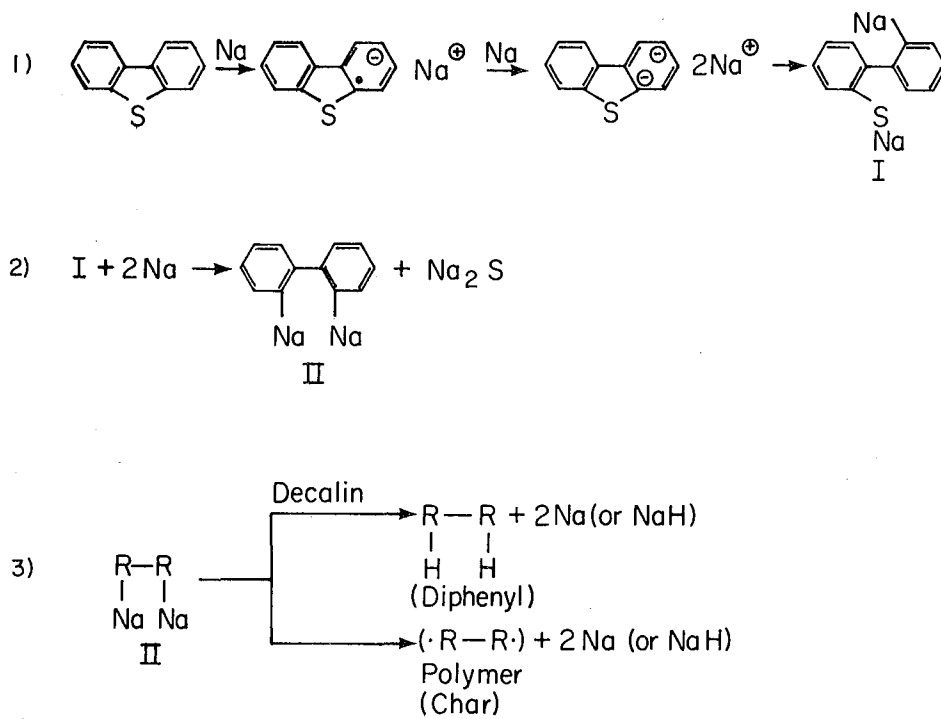
$$-dA/dt = kANa$$

$$\text{where } Na = Na_0 - (A_0 - A)$$

$$\text{and } Na_0 = 3A_0,$$

$$Na/A_0 = 2 + A/A_0.$$

Substitution of $x = A/A_0$ and integration of the above expression yields a simple equation allowing rapid calculation of $k't$ in terms of x :



XBL 795-1502

Fig. 18. Sternberg's mechanism of dibenzothiophene desulfurization. Reproduced by permission of ACS, from "Reaction of Sodium with Dibenzothiophene," *Ind. Eng. Chem., Proc. Des. Dev.* v. B(4) © ACS 1974.

$$\ln((2+x)/3x) = k't$$

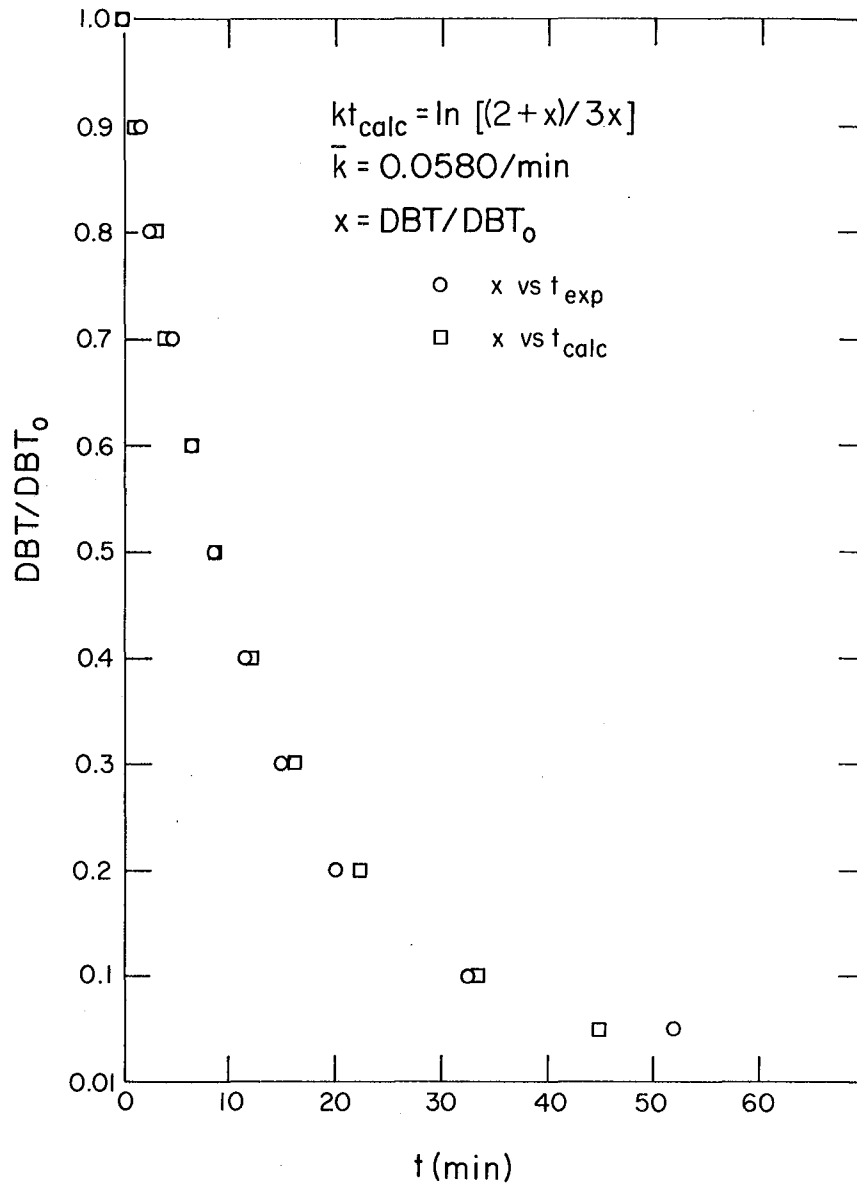
The value of $k't$ is then divided by the corresponding experimental time to yield k' .

Table 15 - Calculation of Experimental Curve of
Dibenzothiophene Concentration vs. Time

<u>x</u>	<u>k't</u>	<u>t_{exp}</u>	<u>k'=k't/t_{exp}</u>	<u>t_{calc}=k't/k'</u>
1.0	0.	0	-	-
0.9	0.0715	1.5	0.0477	1.23
0.8	0.154	2.5	0.0616	2.66
0.7	0.251	4.5	0.0588	4.33
0.6	0.368	6.5	0.0566	6.34
0.5	0.511	8.5	0.0601	8.81
0.4	0.693	11.5	0.0603	12.0
0.3	0.938	15	0.0626	16.2
0.2	1.30	20	0.0650	22.4
0.1	1.95	32.5	0.0599	33.6
0.05	2.61	52	0.0503	45.0

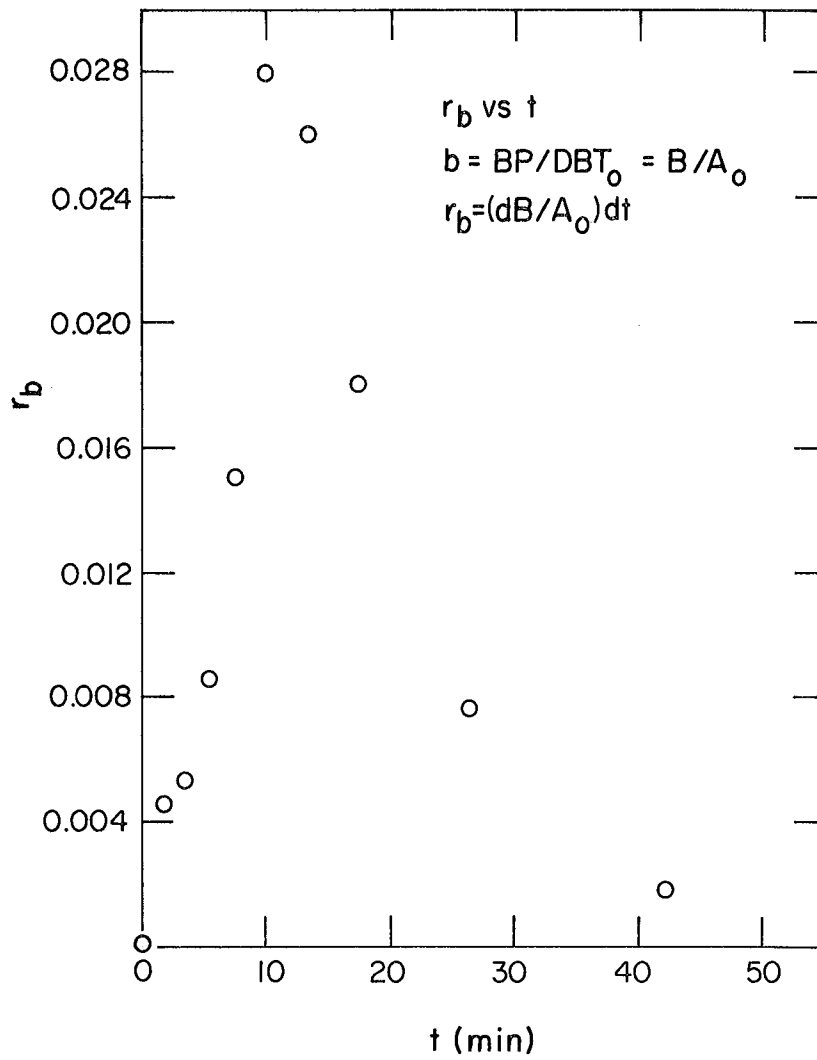
The average value of k' is 0.0580. Using this value, t can be calculated over the range of x , and the results can be plotted against the experimental curve, as is shown in Figure 19.

When the slope of the curve of BP production is plotted as a function of time, the curve in Figure 20 results. The shape of this curve suggests that the rate of formation of BP depends upon an intermediate species whose concentration vs. time curve has the same shape. If this intermediate is assumed to be fairly stable



XBL 795-1500

Fig. 19. Calculated vs. experimental curves of dibenzothiophene concentration vs. time



XBL 795-1499

Fig. 20. Rate of biphenyl formation vs. time

so that it can have some finite concentration, then its concentration-time curve can be calculated from the following mass balance:

$$A_0 = A + B + nC + A^*$$

where A^* is the intermediate, $A = \text{DBT}$, $B = \text{BP}$, and $C = \text{Char}$. Since $B = nC$,

$$A^* = A_0 - A - 2B.$$

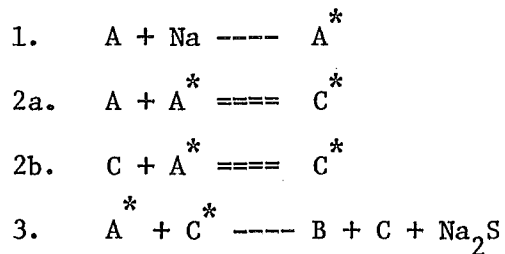
When BP is formed it requires 2 H. Sternberg states that either DBT or solvent (decalin) is the source of this hydrogen. In our experiments we found that the level of tetralin and naphthalene impurities in the solution remained constant with time, indicating no hydrogen-donation by the solvent. Furthermore, Sternberg found that the molecular formula of the char was such that it could have evolved more hydrogen during polymerization than was required in the production of BP, indicating that all the hydrogen required for BP production could have ultimately derived from DBT.

In summary of the preceding discussion, experimental results indicate the following:

1. The rate of disappearance of DBT is first-order in both DBT and Na.
2. The rate of production of BP is proportional to the concentration of a fairly stable intermediate.

3. DBT, upon polymerization to char, releases the hydrogen required in the formation of BP.

These three statements can be translated into the following simplified mechanism:



A = DBT $A^* = DBT^- Na^+$ $C^* = \text{hydrogen-rich char}$
B = BP C = Char

In step 1 a radical anion is formed, as in Sternberg's mechanism. In step 2 this anion polymerizes to form a hydrogen-donating species. Examination of reasonable structures shows that the polymerization must occur at the meta-position to the sulfur (74). In step 3 this species loses its two hydrogen atoms to the anion, which then forms Na_2S and BP.

Equation 1 was written to satisfy the condition that the rate of DBT disappearance was found to be first-order in both sodium and DBT. In addition, it agrees with the first step in Sternberg's mechanism. The solved differential equation and resulting calculations appear on a previous page, while the comparison of calculated and experimental curves of reaction appear in Figure 19.

Equation 2 of the above mechanism is a rapid equilibrium step in

which the hydrogen-rich transient species C^* is formed. The anion A^* can also react with the species C , so an expression for C^* can be written once the following assumptions are made:

1. Concentration of $C^* \approx 0$.
2. $A_0 = A + B + A^* + C$
 $X = \text{Species with which } A^* \text{ polymerizes}$
 $\approx A_0 - A^*$
3. Then $C^* \approx K_2 A^* (A_0 - A^*)$

Equation 3 of the above mechanism was written to satisfy the condition that the rate of appearance of BP is proportional to an intermediate and that the source of hydrogen for the reaction is the DBT.

The rate of reaction of A^* can then be written:

$$\begin{aligned} dA^*/dt &= k_1 ANa - k_3 A^* C^* \\ &= k_1 ANa - k_3 K_2 (A^*)^2 (A_0 - A^*) \end{aligned}$$

$$\text{Since } -dA/dt = k_1 ANa,$$

$$dA^*/dA = k_3 K_2 (A^*)^2 (A_0 - A^*) / k_1 ANa - 1.$$

Let $x = A/A_0$ and $y = A^*/A_0$; then

$$dA^*/dA = dy/dx = ky^2(1-y)/x(2+x) - 1.$$

The constant $k = k_3 K_2 A_0 / k_1$, and can be approximated using the values of x and y at the maximum of the experimental curve of y vs. t :

$$dy/dx = 0$$

$$k = 0.5(2.5)/(0.35)^2(1 - 0.35)$$

$$= 15.7$$

Using $k = 15.7, 19.1,$ and $22.5,$ the differential equation above can be solved using the Euler technique and a step size of $0.1:$

Table 16 - Calculation of Radical Anion Concentration

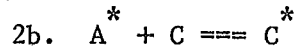
vs. Time Mechanism I

<u>x</u>	<u>t_{exp}</u>	<u>y_{22.5}</u>	<u>y_{19.1}</u>	<u>y_{15.7}</u>	<u>y_{exp}</u>
1.0	0	0	0	0	0
0.9	1.5	0.1	0.1	0.1	0.074
0.8	2.5	0.192	0.193	0.195	0.165
0.7	4.5	0.263	0.268	0.273	0.244
0.6	6.5	0.304	0.316	0.328	0.31
0.5	8.5	0.313	0.334	0.355	0.35
0.4	11.5	0.295	0.324	0.353	0.28
0.3	15	0.254	0.287	0.321	0.20
0.2	20	0.201	0.231	0.262	0.12
0.1	32.5	0.140	0.160	0.181	0.03
0.05	52	0.101	0.116	0.131	0.01

Unfortunately, the curve of y_{calc} does not fit the experimental curve in the region of t greater than $8.5,$ suggesting that the expression for the transient intermediate C^* is incorrect for that region. If it is assumed that two equilibria are involved in the formation of

C^* , the following model results, which is shown in Fig. 21.

$$2a. \quad A^* + A \rightleftharpoons C^*$$



$$C^* = A^* (K_{2a} A + K_{2b} C)$$

$$B = nC$$

$$C^* = K_{2a} A^* (A + kB) \quad (k = K_{2b}/nK_{2a})$$

$$dy/dx = k_1 y^2 (x + k_2 b) / (2 + x)x - 1$$

which compares with the previous equation

$$dy/dx = ky^2(1 - y)/x(2 + x) - 1.$$

The new expression for dy/dx can be solved once the two constants are known. At $dy/dx = 0$, $x = 0.5$, $y = 0.35$, and $b = 0.075$; if values of k_2 are assumed, the corresponding k_1 can be found:

k_2	2.5	5.0	10.0
k_1	14.8	11.7	8.16

The Euler technique can then be used for each set of constants. The results of these calculations are shown in Table 16a; while none of the results fits the experimental curve, the curve resulting from $k_2 = 10$ seems to be nearest in shape.

The last column in Table 16a was calculated using the modified Euler technique, $k_2 = 10$, and $k_1 = 8.16$. This curve still diverges from the experimental curve but provides a better fit than any of the preceding methods. The two curves y_{exp} and y'_{10} are compared in Figure 22.

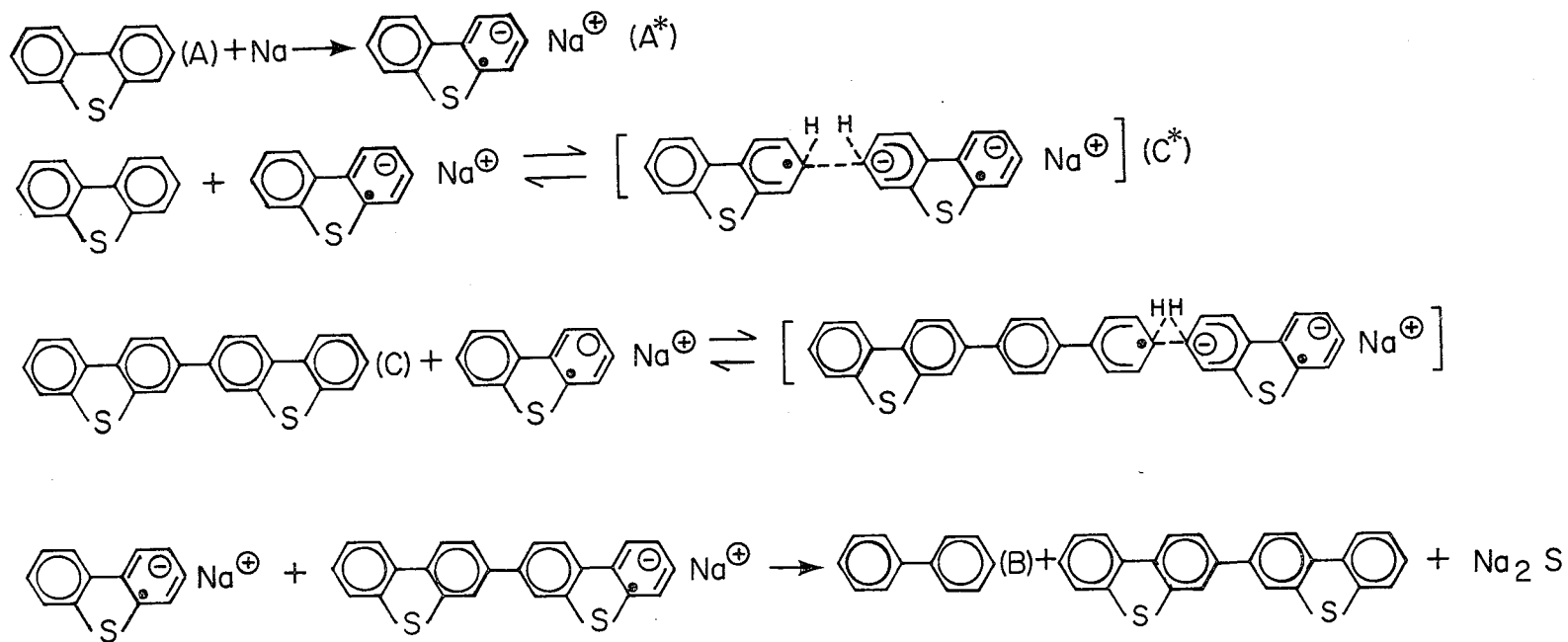
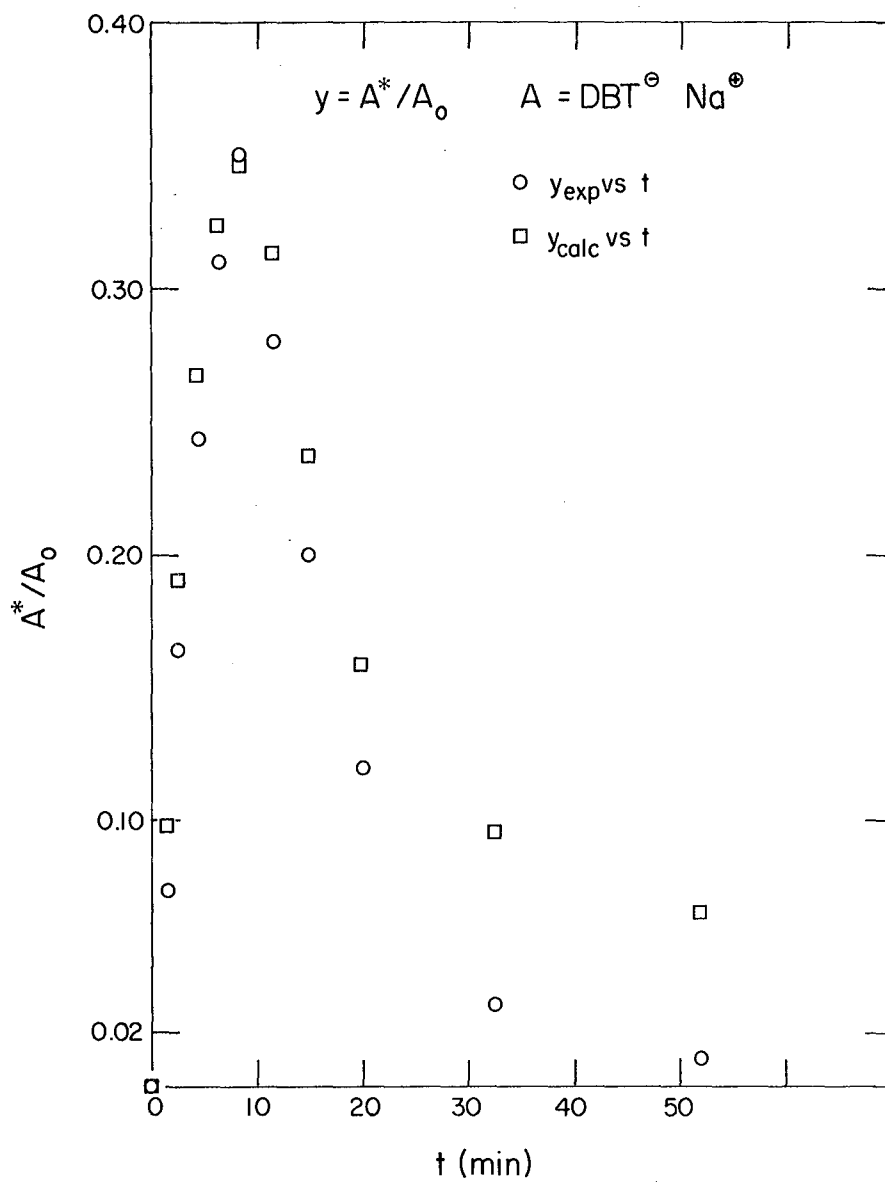


Fig. 21. Proposed mechanism of dibenzothiophene desulfurization

XBL 795-1501

Table 16A - Calculation of Radical Anion Concentration vs.

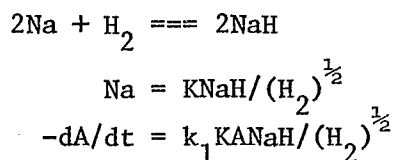
<u>x</u>	<u>Time Mechanism II</u>				
	<u>y_{2.5}</u>	<u>y₅</u>	<u>y₁₀</u>	<u>y_{exp}</u>	<u>y'₁₀</u>
1.0	0	0	0	0	0
0.9	0.1	0.1	0.1	0.074	0.098
0.8	0.195	0.196	0.197	0.165	0.190
0.7	0.274	0.278	0.283	0.244	0.268
0.6	0.328	0.338	0.349	0.31	0.324
0.5	0.355	0.367	0.382	0.35	0.346
0.4	0.352	0.357	0.363	0.28	0.314
0.3	0.298	0.271	0.239	0.20	0.237
0.2	0.221	0.178	0.150	0.12	0.159
0.1	0.148	0.118	0.099	0.03	0.096
0.05	0.106	0.080	0.064	0.01	0.065



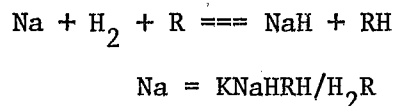
XBL 795-1497

Fig. 22. Calculated vs. experimental curves of radical anion concentration vs. time

Sternberg states that hydrogen inhibits conversion of DBT, possibly due to formation of less reactive NaH. Assuming that a rapid equilibrium is established, then the following applies:



Another possible reaction involving the formation of NaH makes use of the assumption that when H_2 splits, one of the atoms is used to form NaH, while the other atom is captured by some organic species more abundant than Na:



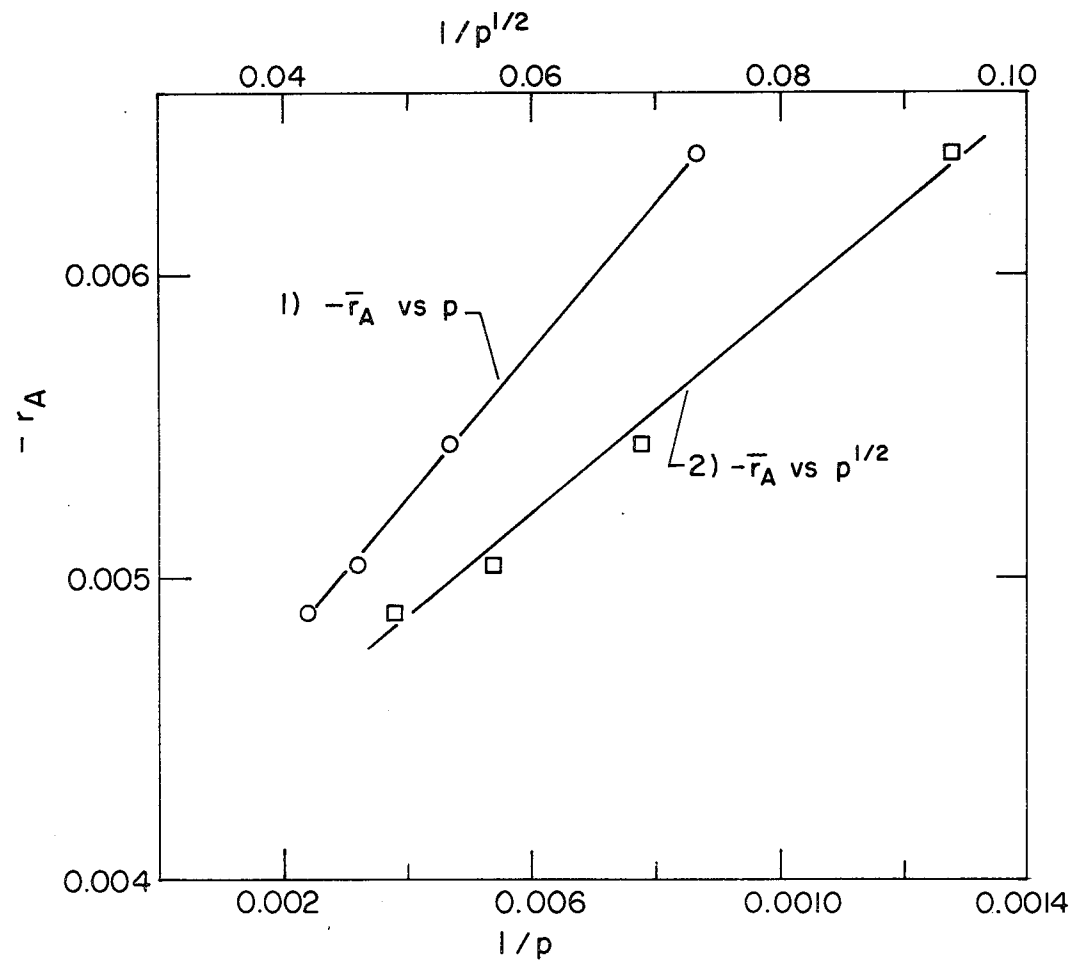
Thus, the first model predicts that the rate of DBT disappearance is $-1/2$ order in H_2 , while the second model predicts that the rate is negative first-order in H_2 . Experimental results are shown in Figure 23, and they agree with the second model.

Table 17 contains values used in plotting experimental curves of $x = A/A_0$, $b = B/A_0$, $y = A^*/A_0$, and $r_b = dB/A_0 dt$ vs. time (t). It should be noted here that the curve of y vs. t was found using the equations

$$A_0 = A + B + nC + A^*$$

$$B = nC$$

$$y = 1 - x - 2b.$$



XBL 795-1498

Fig. 23. Rate of dibenzothiophene reaction vs. hydrogen pressure

Table 17 - Experimental Values Used in Calculations

<u>x</u>	<u>t</u>	<u>b</u>	<u>y</u>	<u>r_b</u>	<u>t'</u>
1.0	0	0	0		
0.9	1.5	0.013	0.074	-	0.75
0.8	2.5	0.0175	0.165	0.0045	2.0
0.7	4.5	0.028	0.244	0.00525	3.5
0.6	6.5	0.045	0.31	0.0085	5.5
0.5	8.5	0.075	0.35	0.015	7.5
0.4	11.5	0.16	0.28	0.028	10.0
0.3	15	0.25	0.20	0.026	13.3
0.2	20	0.34	0.12	0.018	17.5
0.1	32.5	0.435	0.03	0.0076	26.3
0.05	52	0.47	0.01	0.0018	42.3

It can be concluded that the reaction of DBT and sodium depends on the presence of char into which the sulfur is trapped. The advantage of this kind of mechanism is that sulfur is concentrated in the non-volatile residue of a coal-liquid desulfurization process, and is thereby prevented from contaminating more volatile and saleable distillates.

C. Coal and Coal-Derived Materials

Solid SRC in decalin formed the substrate for the next series of runs. A dispersion of 100 mesh SRC in decalin was reacted for 2-3 hours with

sodium dispersion, then washed with 0.5 M HCl to remove the sodium from the SRC matrix. The SRC was filtered from the decalin and analyzed for percent sulfur remaining. The results are shown in Table 18.

Table 18 - Reaction of Solid SRC and Coal with Sodium

<u>RUN</u>	<u>COMMENTS</u>	<u>Per Cent Sulfur</u>
SRC-12	React w/Na; HCl Wash	0.17
-13	React w/Na; HCl Wash	0.35
-14	React w/Na; HCl Wash	0.21
-15	React w/Na; HCl Wash	0.05
-16	HCl Wash Only	0.42
-17	React w/Na; HCl Wash	0.18
-18	React w/Na; HCl Wash	0.19
-19	HCl Wash Only	0.69
SRC	No Reaction or Wash	0.69
IN6-1	React w/Na; no wash	2.43
-2	HCl Wash Only	2.51
-3	React w/Na; HCl Wash	1.94
-4	HCl Wash Only	2.79
-5	React w/Na; HCl Wash	2.90
IN6	No Reaction or Wash	3.54

Conditions for these runs were 200° C and 100 psig H₂. The H₂ was used

in hopes of shifting equilibrium production in the direction of H_2S .

Table 18 includes results with several runs of Illinois #6 (IN6) coal. Conversion was very poor in these runs so they were discontinued. The runs with SRC, however, showed fairly good desulfurization. Since neither the decalin solution nor the HCl wash was tested for sulfur, and since only a negligible amount of H_2S was absorbed after the HCl wash in each case, it is assumed that the sodium concentrated with sulfur in a high-sodium, high-sulfur char, which was then extracted by the HCl wash. If Na_2S had been formed, then substantial amounts of H_2S would have been collected by the absorber. Conversely, if the high-sulfur char had remained with the filtered SRC, the per cent sulfur should have remained unchanged from the blank runs.

Finally, runs of undiluted SRC recycle slurry were carried out to see if sodium was able to concentrate the sulfur in a separable residue. Recycle slurry was weighed, then heated to $60^\circ C$, and added to a three-necked flask as described earlier. Sodium dispersion was added, and the mixture was stirred for two to three hours, then distilled under -27 in Hg pressure to a temperature of $240^\circ C$. The residue and distillate were weighed and tested for %C,H,N,Na,S, and ash. Results are presented in Tables 19, 20, and 21.

In Table 19 are given per cent sulfur in the distillate (S_v), per cent sulfur in the bottoms (S_1), and per cent sulfur in the bottoms that was converted to SO_2 during combustion of the samples (S_{SO_2}). Per cent ash and sodium are also given for the bottoms product.

Table 19 - Sulfur Distribution Resulting from Reaction
of Sodium with SRC Recycle Slurry

<u>Run</u>	<u>S_v</u>	<u>S_l</u>	<u>S_{SO₂}</u>	<u>Ash</u>	<u>Na</u>
20	0.43	1.32	1.31	6.9	0,288
24	0.23	1.27	0.21	21.5	6.03
25	0.14	1.23	0	29.0	8.03
26	0.09	1.03	0	33.1	10.7
27	0.05	1.04	0.03	20.1	4.53
28	0.22	1.28	1.24	5.9	0.309
29	0	1.04	0.04	-	8.21

Table 20 - Vapor-Liquid Distribution Resulting from Reaction
of Sodium with SRC Recycle Slurry

<u>Run</u>	<u>F</u>	<u>V</u>	<u>L</u>	<u>V/(V+L)</u>
20	86.53	30.17	57.13	0.346
24	181.92	64.04	118.38	0.351
25	82.98	45.41	47.15	0.491
26	75.40	44.33	50.40	0.468
27	116.04	49.80	85.20	0.369
28	140.30	45.15	92.00	0.324
29	79.32	27.23	67.70	0.287

In Table 20 are given mass balances for each distillation, in terms of amount of slurry fed (F), amount of distillate (V), and amount of bottoms or residue (L).

Table 21 - Average Values of Sulfur and Vapor-Liquid Distribution

	$V/(V+L)$	$L/(V+L)$	S_v	S_1	S_{SO_2}	Ash
Blank	0.3375	0.6625	0.325	1.30	1.275	6.4
Na	0.3932	0.6068	0.07	1.122	0.038	25.9

In Table 21 are given average values compiled from Tables 19 and 20. Runs with sodium are indicated by "Na". Fractions of distillate and bottoms are corrected for the presence of a volatile dispersing agent (decalin) and a non-volatile dispersing agent (mineral oil), which distribute into the vapor and liquid phases, respectively.

These results indicate that the sodium treatment decreases the amount of sulfur in the distillate by 78% and a mass balance around an SRC vacuum distillation stage reveals that sulfur is retained in the residue. Moreover, the sodium acts to reduce SO_2 emissions upon burning the residue. Burning 100 lb. of untreated experimental vacuum residue releases 2.55 lb. of SO_2 , while burning the same amount of treated residue releases only 0.076 lb. SO_2 . This 97% reduction in SO_2 emission is much greater than would be required by EPA's new source standards. Thus while the untreated residue cannot be burned without costly FGDS facilities, treated residue can be burned without further cleaning. This property is important to the SRC process because the treated residue can be used for process heat and steam generation in the SRC process, thus shifting the burden of heat generation away from more saleable fuels.

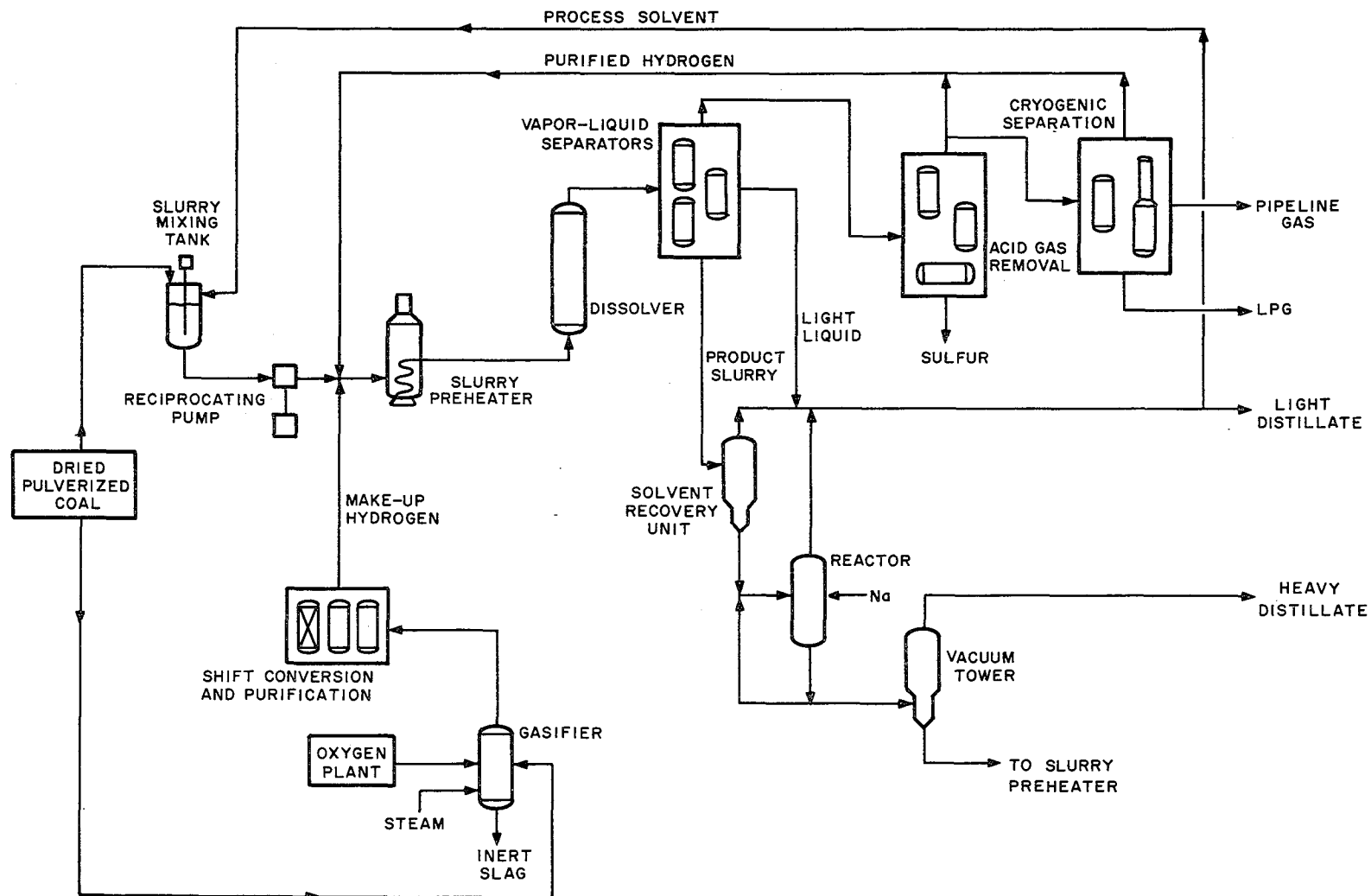
IV. APPLICATIONS

A. Modified SRC Process

Figure 24 gives the flow diagram for a modified SRC recycle solvent process that includes a sodium treatment step. Figure 25 gives flow diagram and mass balance for an unmodified recycle solvent process.^{74,75} The primary differences between the two are that the vacuum bottoms is gasified in the unmodified process, and that the vacuum bottoms is burned in the modified process.

Figures 26 and 27 compare the changes in the flow of sulfur as calculated from the results in Table 21. In Figure 26 is shown the fate of the atmospheric bottoms from the SRC process. The vacuum distillation produces a fuel oil which, when burned, produces SO_2 within limits allowed by the EPA new source standards. However, when the high-sulfur residue from this step is burned, it produces SO_2 in amounts 15 times higher than allowed.

In Figure 27 is shown the treatment of the atmospheric bottoms (A.B.) with sodium. The mass flows in this diagram were calculated on the basis of Table 21, using a minimum amount (3.8%) of sodium in a 60% fuel oil (F.O.) dispersion. The sodium treatment increases the fuel oil production by 8% and yields a substantially cleaner liquid. When this oil is burned, it produces proportionately less SO_2 than is produced by the fuel oil from the unmodified process. The key point, however, is that when the modified process residue is burned, it also



-71-

Fig. 24. Modified SRC process

SRC RECYCLE SOLVENT PROCESS

XBL 795-1619

SRC MASS FLOWS

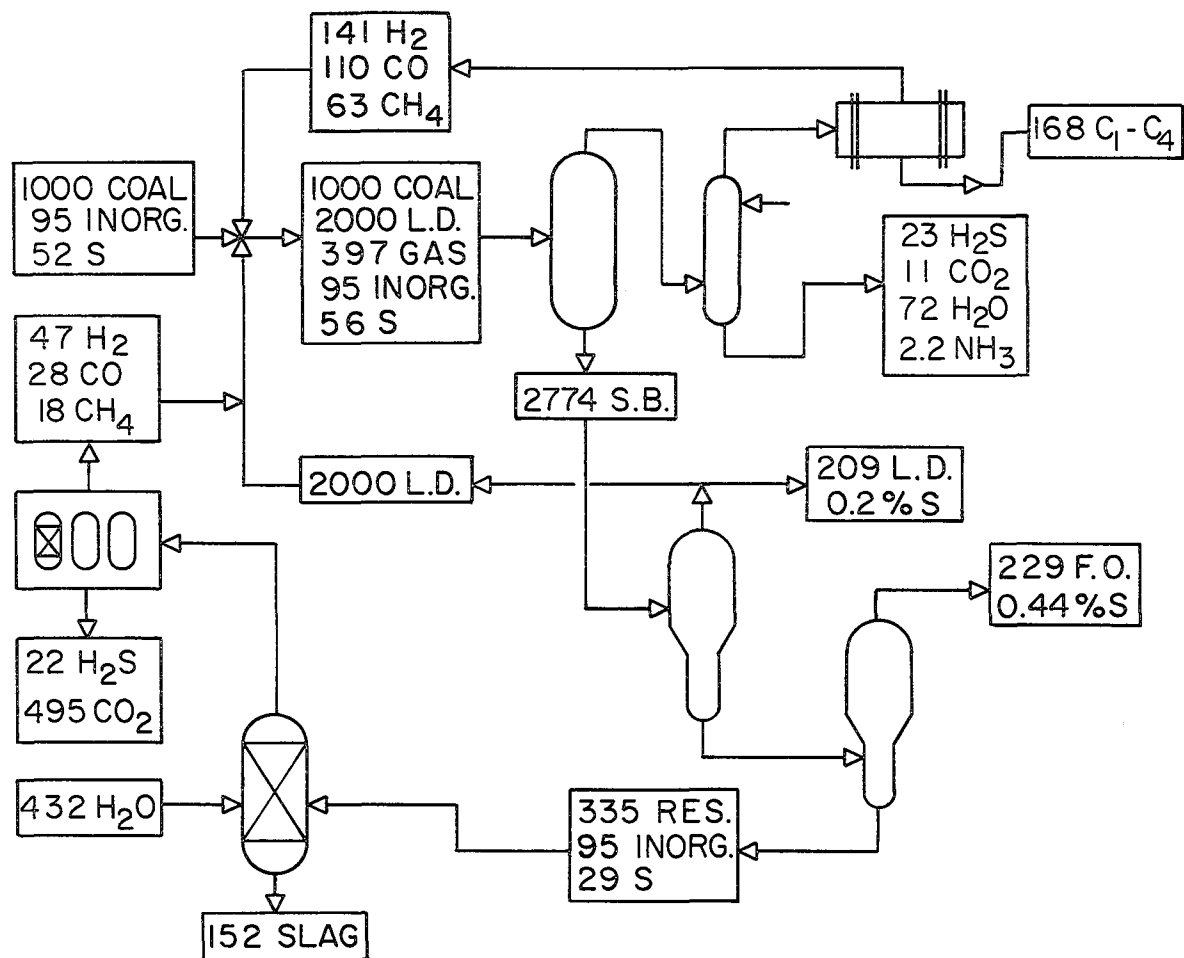


Fig. 25. SRC II mass flows

XBL 795-1519

SRC PROCESS FLOWS

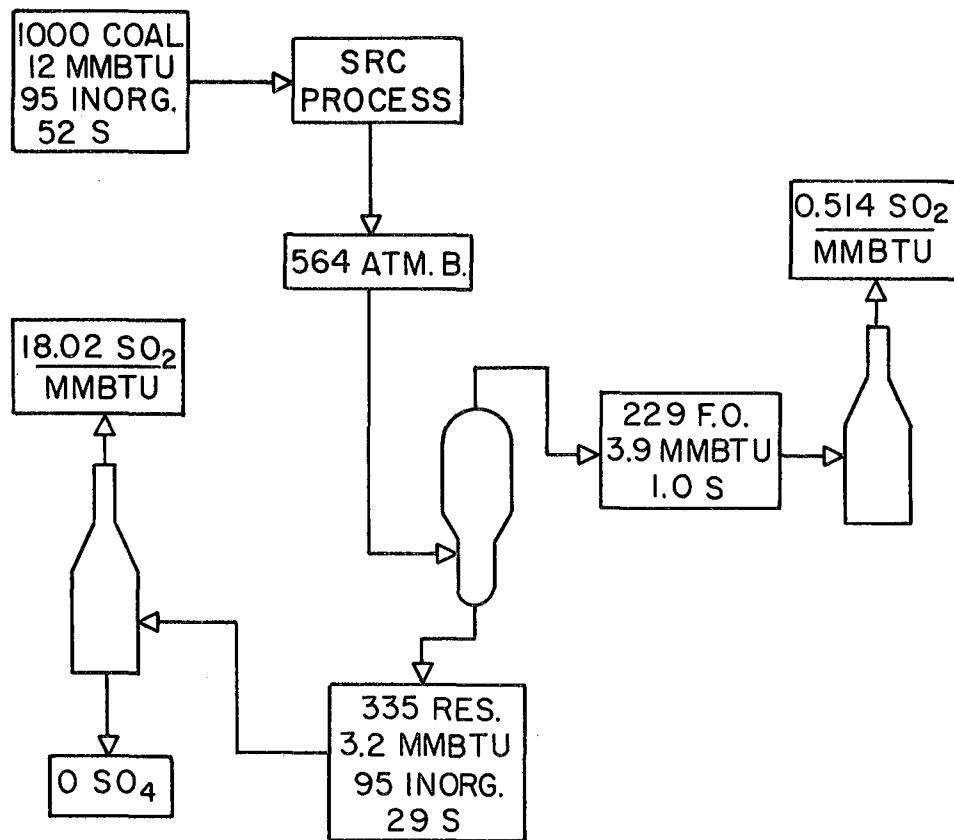


Fig. 26. SRC II atmospheric bottoms of flows

MODIFIED PROCESS FLOWS

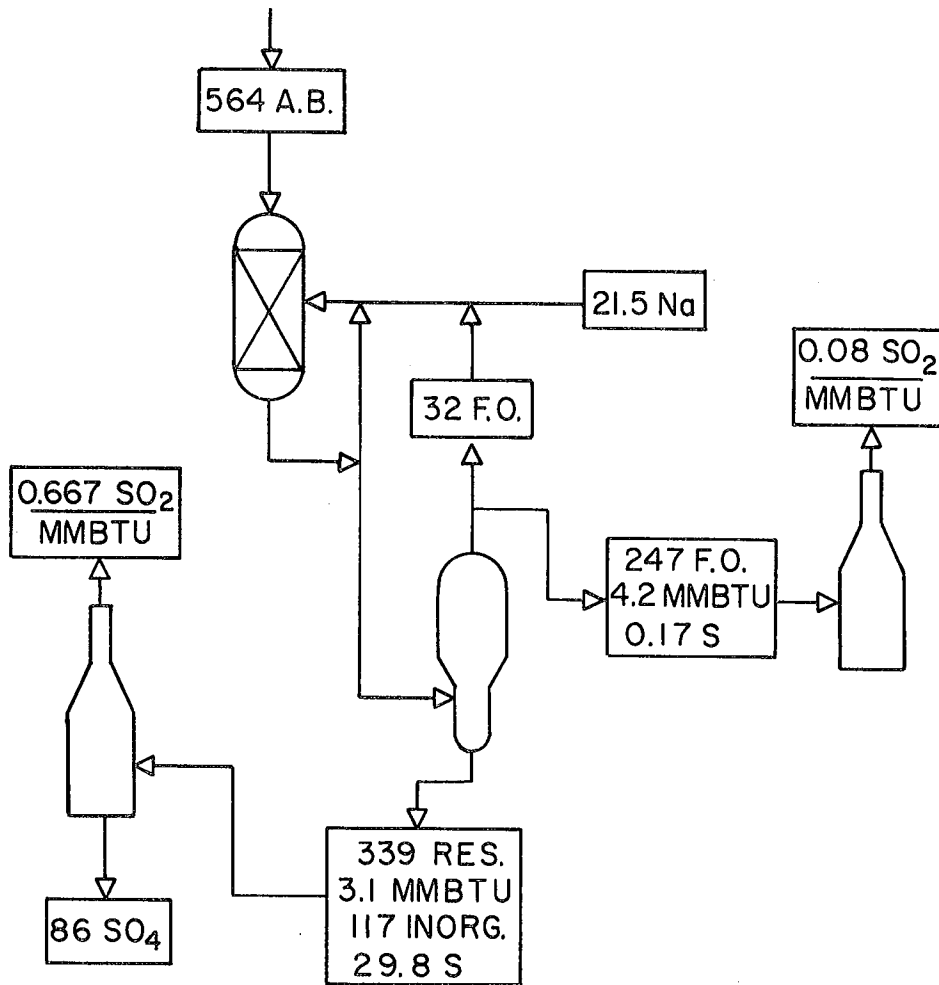


Fig. 27. Modified process atmospheric bottoms flows
XBL 795-1620

produces SO₂ well within EPA limits. Thus, the sodium treatment can be used to shift burning away from clean but saleable fuel oil towards unsaleable vacuum residue.

Thus, the function of sodium in the reaction with SRC recycle seems to be conversion of volatile organic sulfur into more volatile desulfurized product and high-sulfur char. The sodium remains associated with the sulfur in the char, so that when it is burned, the sulfur is trapped as sulfate. A number of metals do something similar, as is shown in the table below, which gives sulfate decomposition temperatures for alkali metals and earths.^{76,77}

Table 22 - Sulfate Salt Decomposition Temperatures				
Reaction:	$\text{MeSO}_4 = \text{MeO} + \text{SO}_2 + \frac{1}{2}\text{O}_2$			
Salt	Na ₂ SO ₄	K ₂ SO ₄	CaSO ₄	MgSO ₄
MW	142	174	137	120
$\Delta G_{R,298}^\circ$	141.10	149.42	99.48	72.69
$\Delta H_{R,298}^\circ$	160.56	185.32	119.58	90.72
$\ln K_{R,298}^\circ$	-236.74	-250.70	-166.91	-121.96
$\ln K_{R,T}^\circ$	-4.96	-5.16	-4.92	-4.79
T _{exp}	-	-	1200 C	972° C
T _{calc}	1860° C	1143° C	1273° C	1021° C

The decomposition temperatures are calculated on the basis that the samples are being burned for 15 minutes in a flow of 10 ml/min O₂ at 14.7 psia with a sample size (sulfate salt) of 10 mg. The reaction $\text{MeSO}_4 \rightleftharpoons \text{MeO} + \text{SO}_2 + \frac{1}{2}\text{O}_2$ has an equilibrium constant $K = Y_{\text{SO}_2} Y_{\text{O}_2}^{1/2} p^{1.5}$, since $a_{\text{MeSO}_4} = a_{\text{MeO}} = 1$. K further reduces to $K = Y_{\text{SO}_2}$, since O₂ makes up most of the atmosphere in the furnace, which is at atmospheric pressure. Since the total moles of O₂ = 0.01 during the combustion of the sample, and since the number of moles of sulfur is .01/MW salt, $Y_{\text{SO}_2} = (0.1/\text{MW})/0.01$, or $1/\text{MW}$. Since

$$\ln K_T = \ln K_{298} + (\Delta H_{298}/R)(1/298 - 1/T),$$

$$T_{\text{decomp}} = 1/(1/298 - (R/\Delta H_{298})(\ln(K_T/K_{298}))).$$

This temperature is that to which the furnace must be raised to insure complete decomposition of a 10 mg. sample of the sulfate salt.

Table 23 - Relative Volatilities of Reactants and Products in Hydrodesulfurization Reactions

<u>Reactant</u>	$\frac{P_r^0}{r}$	<u>Product</u>	$\frac{P_p^0}{p}$	$\frac{P_p^0}{P_r^0}$
Diethyl Sulfide	12 atm.	Ethane	30.99 atm.	2.58
Thiophene	2.73 atm.	Butadiene	9.38 atm.	3.44
Benzothiophene	530 Torr.	Ethyl Benzene	1499 Torr	2.83
Diphenyl Sulfide	188 Torr	Diphenyl	230 Torr	1.22
Dibenzothiophene	64 Torr	Diphenyl	230 Torr	3.59
Thianthrene	20 Torr	Diphenyl	230 Torr	11.5

T = 200°C

The function of sodium in conversion of sulfur compounds into more volatile desulfurized products is illustrated in Table 23.^{78,79} When the sodium-treating step is followed by an equilibrium flash or distillation, the overall effect of sodium treatment is to increase both the purity and amount of distillate.

B. Modified SRC Process Economics

Existing technology in coal desulfurization amounts to either separation of pyrites or flue-gas desulfurization. Of the two, only flue gas desulfurization can meet EPA standards for most coals.

Comparison of scrubbing costs with sodium cleanup of a recycle SRC is therefore in order, and is given in Tables 24 and 25.^{71,75,80}

Since flue gas scrubbing is only a cleanup process, no credits or savings can be assigned to it, and only a cost per ton of coal can be used as a parameter of comparison. In the case of the sodium treatment, a cost per ton of residue can be assigned only if the fuel oil credit is ignored. Using this technique, the cost of the sodium process is \$52.74 per ton residue, which is clearly not competitive with scrubbing. Only if the fuel oil credit is allowed does the sodium process become economical.

This sort of analysis ignores the fact that fuel oil appreciates in value with decreasing sulfur content. For example, Table 26 lists various petroleum-derived fuel oils, their current prices, and sulfur contents.⁸¹ The cleanest oil is most valuable, and the extra value

Table 24 - Flue Gas Scrubbing Costs

Scrubber	Installed Cost	Capital Cost	Total Operating Cost	
Lime-Limestone	\$ 60/KW	0.75 mil/KWH	3.0 mil/KWH	\$ 8.48/ton coal
Reduction-Recycle	\$250/KW	3.0 mil/KWH	8.0 mil/KWH	\$22.50/ton coal

Costs are given for a 10^6 KW coal-fired plant using 8532 ton/day of coal. Straight-line depreciation over ten years, no salvage value, and 8000 hr/yr operating time are assumed.

Cost increments for a 25246 ton coal per day SRC plant are tabulated below. Total capital investment is 1 billion dollars. 25246 tons/day of 500 psi steam are required, at \$6/ton. 8532 tons/day residue are produced, with a heating value of 16251 MMBTU. Coal is priced at \$24 per ton. Costs and credits are given in thousands of dollars per day.

Table 25 - Changes in SRC Economics Due to Sodium Treatment

Cost or Credit	Without Na	With Na	Comments
Fuel Oil for Process Heat or Steam Gen.	-556.7	-	60590 MMBTU/day Process Heat 58870 MMBTU/day Steam Gen. Fuel Oil at \$4.66/MMBTU
Steam Credit	-	+110.8	Res. has more H. V. than above.
Extra Fuel Oil	-	+72.2	Na treatment yields 8% more fuel oil.
Coal to gasifier	-	-97.6	Replace res. with coal as gasifier feed.
Na cost	-	-444.9	543 ton/day @ \$820/ton
Na process Installed cost	-	\$60* 10^6	Same as lime-limestone scrubber cost.
Na capital cost	-	-18.1	$8532*8.48*0.75/3.0$
Na labor, maint., etc.	-	-72.4	Cap. Cost*4
Total	-556.7	-450.0	
Net Saving		106.7	

Since 6236 tons/day fuel oil are produced, with a previously required selling price of \$25/bbl or \$159/ton, the new price could be $(6236*159 - 106700) / 6236$, or \$22.35 per barrel.

can be assigned almost entirely to scrubbing costs. For example, using a scrubbing cost of \$8.48 per ton coal, or \$0.353 per million BTU, and starting with a dirty fuel oil at \$12.75 per barrel and 5.76 million BTU per barrel, the incremental lime-limestone scrubbing cost is \$2.04 per barrel. When this is added to the cost of the dirty fuel oil, a new value of \$14.79 per barrel results, similar in magnitude to the actual price of clean fuel oil.

Table 26 - Effect of Sulfur Content on Fuel Oil Value

<u>Fuel Oil</u>	<u>Sulfur Content</u>	<u>Price per Barrel</u>
#6	2%	\$12.75
#6	0.3%	\$13.70 to \$14.53
#5	0.3%	\$14.30 to \$15.08

Therefore, since the sodium process results in an SRC-derived fuel oil that is 80% cleaner than the same fuel oil without sodium treatment, it is reasonable to expect that the sodium treatment also upgrades the value of the fuel oil.

C. Co-Combustion Process for Coal Cleaning

The tendency of sodium to form Na_2SO_4 upon combustion suggests a process involving the contacting of molten NaOH with coal, and the subsequent burning of the mixture.

Addition of 1 g. NaOH to 10 g. Illinois #6 coal and subsequent combustion at 850°C for 15 min. in an O₂ furnace yields an approximate distribution of sulfur as 20% SO₂ and 80% Na₂SO₄. Both coal and NaOH were of 100 mesh size.

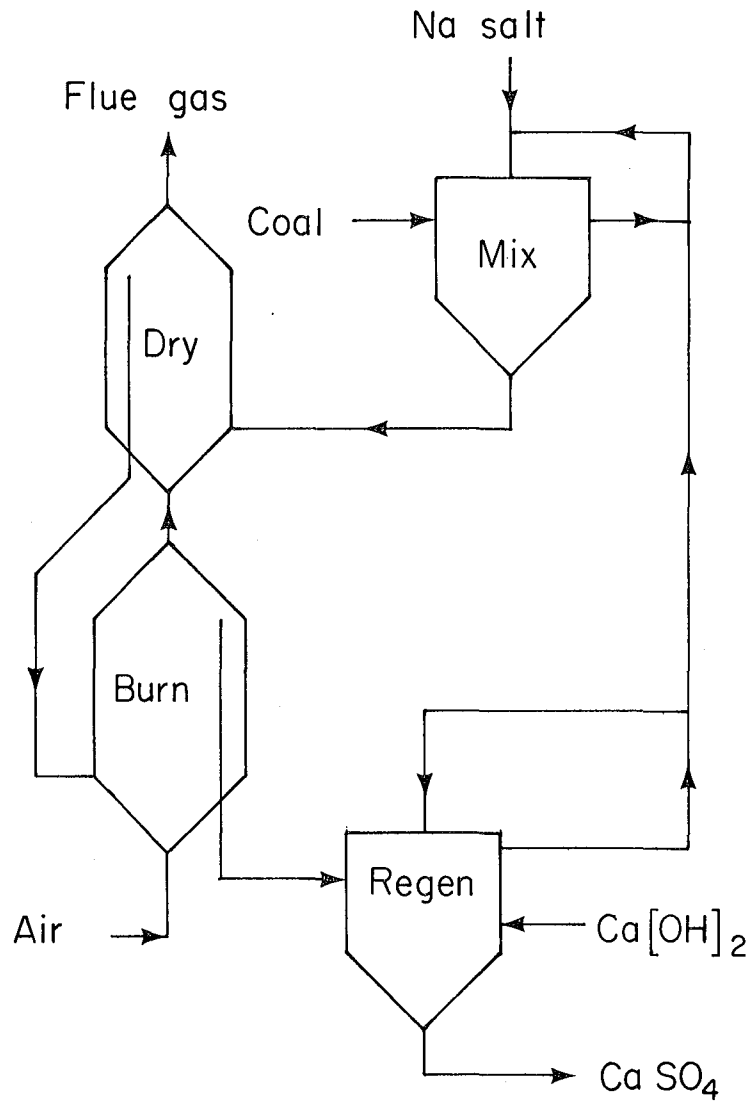
NaOH was selected for three reasons::

1. It is very water-soluble, allowing better coal-contacting than an insoluble salt.
2. It has a low (330°C) melting point, allowing fusion and good penetration of coal particles at low temperatures prior to combustion.
3. Its sulfate product has the highest decomposition temperature (lowest SO₂/O₂ equilibrium) of any sulfate salt.

A process involving combustion of coal with a sodium salt is described in Figure 28. The unit operations are coal-salt contacting, drying, combustion, and sulfate regeneration.

The first stage in the process is mixing of coal and 20 wt.% salt solution, at room temperature and atmospheric pressure. The solution is separated from the coal and, saturated in humic acids, recycles to the mixing process. The wet coal mixture, approximately 1/2 coal and 1/2 solution, is fed to a fluid bed drier. The mixture, dried by furnace exhaust gases, traps any residual SO₂ or fly ash in the exhaust. The overflow from the dryer is fed to a fluid bed furnace, where salt is converted to sulfate as coal is burned. The ash is either discarded or leached of sulfates, which are then regenerated to reactive salts

Co-combustion process



XBL 795-1503

Fig. 28. Co-combustion process

by contact with a lime solution.

Tests were carried out to see what salts could be used as sulfur-trapping agents. The criteria for selection were low cost and high solubility in H_2O . In each case, IN6 coal (3.54% S) was wetted with a 20% solution and dried overnight. Results are presented in Table 26A.

Table 26A - Sulfur Retention by Sodium Salts

<u>Salt</u>	<u>% S Retained in Ash</u>	<u>% S Converted to SO_2</u>
NaOH	97	3
Na_2CO_3	99	1
Na_2SO_3	48	52

The reaction expected for Na_2SO_3 was conversion to $NaHSO_3$, which was apparently inhibited by the large excess of O_2 present in the analytical furnace.

In Tables 24, 27, 28, and 29 are presented rough cost data for various processes. In Table 27, the unit operating costs for Meyers oxidative ferric sulfate leach process and the co-combustion process are compared. Cost data were obtained from a comprehensive preliminary economic design report prepared by Dow Chemical Co. on a commercial-scale Meyers process desulfurization unit.⁸² Certain costs are estimated to be halved or eliminated in the co-combustion process because conditions

COMPARISON OF COSTS BETWEEN MEYERS PROCESS AND CO-COMBUSTION

Table 27 - Operating Costs, 1979 \$/Ton Coal

Unit	Meyers	Co-Combustion	Comments
Coal Handling	4.81	2.41	Same amount of drying No compaction No binders Much less crushing
Leaching	6.38	3.19	Coal contacting only No mass-transfer problems Ambient T & P
Extraction	3.63	-	No extraction
SO ₄ Disposal	3.24	3.24	Similar sulfate problem
Total	18.06	8.84	
Mil/kwh	6.42	3.14	8532 ton/day = 10 ⁶ kw

Table 28 - Installed Costs, 1979 10⁶ \$, 10⁴ ton/day Capacity

Coal Handling	38.46	23.67	X(0.5) ^{0.7}
Leaching	70.43	43.35	X(0.5) ^{0.7}
Extraction	50.81	-	
SO ₄ Disposal	36.10	36.10	
Total	195.80	103.12	
\$/kw	167	88	

Table 24

Scrubber	Installed Cost	Capital Cost	Total Operating Cost	
Lime-				
Limestone	\$ 60/KW	0.75 mil/KWH	3.0 mil/KWH	\$ 8.48/ton coal
Reduction-				
Recycle	\$250/KW	3.0 mil/KWH	8.0 mil/KWH	\$22.50/ton coal

Table 29 - Chemical Coal Cleaning Costs

Process	Case	Hazen	KVB	Battelle	TRW (Meyers)	LOL	BOM/ERDA
Clean Coal Produced, * (Dry Basis)	T/D	NA	5500	6900	6700	7600	7200
Installed Plant Cost, MM\$	A	13.9	33.9	70.2	97.7	122.0	97.3
Installed Plant Cost, MM\$	B	47.9	67.9	103.4	130.9	155.2	130.5
Net Operating Cost, \$/T (Clean Coal Basis)	A	7.0-25.6	17.0	16.1	13.8	13.2	14.1
Net Operating Cost, \$/T (Clean Coal Bases)	B	14.5-33.1	23.0	21.9	18.9	18.6	19.5

* 8000 T/D ROM Coal Feed, 2.8% moisture

Case A - Desulfurization only

Case B - Including coal prep., desulfurization, and coal compaction

From Ergun (Ref. 84).

are much less severe, steps are much less intense, or steps are eliminated altogether.

In Table 28 installed capital costs for the two processes are compared. Where an operating cost was halved in the previous table, the corresponding installed cost is reduced by the same factor to the 0.7 power.⁸³

Comparison of costs per kw and per kwh show that while both Meyers and co-combustion compete well with the most sophisticated flue-gas scrubbing techniques available, only the co-combustion process competes favorably with the more widely practiced lime-limestone scrubbing system.

Table 29 is provided⁸⁴ to show that most leaching operations have costs similar to those of the Meyers process, so that none of them compete well with the more effective co-combustion or lime-limestone scrubbing processes.

One of the questions that could arise concerning this process is whether the reaction of sodium sulfate to sodium hydroxide is thermodynamically or kinetically favorable. An industrial process has been proposed concerning this reaction,⁸⁵ which is also an integral part of the Battelle caustic leach process,⁸⁶ and the following experiment was carried out to test actual conversion to NaOH. A mixture of Na_2SO_4 and $\text{Ca}(\text{OH})_2$ were stirred overnight in a 500 ml three-necked flask at room temperature. The resulting suspension was then filtered. A fraction of the liquid was titrated with BaCl_2 and the resulting BaSO_4 precipitate

was weighed. This precipitate amounted to 81.5% of the total possible precipitate, had no conversion occurred. The solid product was weighed and analyzed for per cent sulfur, and yielded sulfate equivalent to 28.5% conversion to gypsum (CaSO_4). It is possible that conditions can be found to increase conversion; in any event, Na_2SO_4 in the recycle stream should not effect the overall process of coal cleaning.

V. CONCLUSIONS

Metallic sodium is effective in conversion of volatile organic refractory sulfur into volatile desulfurized products and non-volatile sulfur-bearing species. This fact, in combination with retention of sodium in the char, suggests the use of sodium to treat thiophenic fuel mixtures prior to distillation. The resulting distillate is greatly reduced in volatile organic sulfur. Since the residue retains sodium, it can be burned within EPA limits, because the sodium retains sulfur as SO_4 . Sodium treatment of SRC vacuum distillation feed may be a way of decreasing overall costs in the SRC process.

Due to its tendency towards a number of competing reactions, sodium is not a useful analytical agent for the determination of refractory organic sulfur in fuels. Analysis of extracted sulfur compounds is also out of the question, due to the wide range of products arising from reaction of sodium with any given refractory organic sulfur compound.

VI. ACKNOWLEDGEMENTS

I am grateful for the patience and support of Profs. Petersen, Vollhardt, and Vermeulen and the able assistance of various chemical engineering graduate students, technicians, and administrative personnel, too numerous to mention.

This work was done under the auspices of the U. S. Department of Energy.

VII. REFERENCES

1. Anon., Position Paper on Regulation of Atmospheric Sulfates, EPA 450/2-75-007, Sept. 1975.
2. Ferris, B. G., M. D., "Health Effects of Exposure to Regulated Air Pollutants", JAPCA 28 (5), May 1975, pp. 482-97.
3. Heck, W. W., and J. A. Dunning, "Response of Oats to SO₂", JAPCA 28 (3), March 1978, pp. 241-6.
4. Fishelson, G. and P. Graves, "Air Pollution and Morbidity", JAPCA 28 (8), August 1978, pp. 785-9.
5. Shinn, J., "Anthropogenic Impact on Sulfur Cycle in Northeast United States", paper to be published in 1979.
6. Anon., "Electric Utility Steam-generating Units", Fed. Reg. 43 (182) Part V, Sept. 19, 1978, pp. 42154-84.
7. Lisauskas, R. A. & S. A. Johnson, "NO_x Formation during Gas Combustion", CEP, August 1978.
8. Private Communication, Professor Scott Lynn, U. C. Berkeley.
9. Himmelblau, D. M., Basic Principles and Calculations in Chemical Engineering, Prentice Hall, Inc., 1974, 300 pp.
10. Smith, J. N. & H. C. Van Ness, Introduction to Chemical Engineering Thermodynamics, McGraw-Hill, New York, 1975, 500 pp.
11. Greer, R. T., "Coal Microstructure and Pyrite Distribution", In Coal Desulfurization (Wheelock Ed.) ACS Symp. Ser. 64 (1977).
12. Private Communication, James Mesher, U. C. Berkeley.
13. Gluskoter, H. J., "Inorganic Sulfur in Coal", ACS Fuel Chem. Div. v. 20 (2), p. 94 (1975).
14. Paris, B., "Organic Sulfur in Coal", in Coal Desulfurization (Wheelock Ed.).
15. Kuhn, J. K., "Forms of Sulfur in Coal", Ibid.

16. Shimp, N. F., et al., "Determination of the Forms of Sulfur in Coal", ACS Fuel Chem Div v. 20 (2), p. 99 (1975).
17. Murray, H. H., "Magnetic Desulfurization of Coal", in Wheelock, Op. Cit.
18. Mendizabal, E., Low Temperature Processes for Coal Desulfurization, M. S. Thesis, U. C. Berkeley, August 1976.
19. Emmett, P. H., in Mendizabal, Op. Cit.
20. Powell, A. R., "Study of the Reactions of Coal Sulfur", J. Ind. Eng. Chem. 12, p. 1069 (1920).
21. Anon., "Qualitative Determination of Sulfur-compounds in Turkish Coals", Istanbul Tek. Univ. Bull. 24 (1), pp. 28-52 (1972). In Chem. Abstr. 5567u 76 (1972).
22. Fine, D. H. & J. B. Westmore, "Heat of Formation of Various Radicals", Chem. Commun. 1969 (6) p. 273.
23. Hill, G. R. & L. B. Lyon, Ind. Eng. Chem. 54 (6), June 1962.
24. Wiser, W. H., "Coal Catalysis", Proc. of EPRI Conf., Sept. 1970.
25. Meyer, V., Die Thiophengruppe, Braunschweig 1888.
26. Byrns, A. C. et al., Ind. Eng. Chem. 35, p. 1160 (1943).
27. Casagrande, R. M. et al., Ind. Eng. Chem. 47, p. 744 (1955).
28. Hartough, H. D., Condensed Thiophenes, Interscience Pub., Inc., New York, 1954, 500 pp.
29. Lowry, H. H., Ed., Coal Utilization, J. Wiley & Sons, New York, 1963, 1142 pp.
30. Boes, J., Apothekerst 17 p. 565 (1902), In Hartough, Op. Cit.
31. Weissgerber & Kruber, in Hartough, Op. Cit.
32. Weissgerber & Kruber, Brentsdorff Chem. 2 p. 1 (1921). In Hartough, Op. Cit.

33. Kruber, Ber B53, p. 1566 (1920), in Hartough Op. Cit.
34. Cusev, J. App. Chem. (USSR) 17, p. 178 (1944).
35. Hoog, Rec Trav Chim 69, p. 1289 (1950).
36. Oae et al., "Rearrangement of Diphenyl Sulfide", Chem Ind 45, p. 1438 (1970).
37. Aitken, J. et al., "Organic Sulfur in Coal", Fuel 47, p. 353 (1965).
38. Landa, S. and A. Mrnkova, "Hydrogenation of Organic Sulfur Compounds", Chem., Abstr. 67, 13492v (1967).
39. Hayatsu, R. et al., "Aromatic Units in Coal", Nature p. 257 (Oct. 2, 1975).
40. Hayatsu, R. et al., "Trapped Organic Compounds in Coal", Fuel 57 p. 541 (Sept. 1978).
41. Benson, S. W., Thermochemical Kinetics, J. Wiley & Sons, New York 1968, 223 pp.
42. Benson, S. W. et al., "Additivity Rules for the Estimation of Thermochemical Properties", Chem. Rev. 69, p 273 (1969).
43. Wheelock. Op. Cit.
44. Ergun, S. et al., Analysis of Chemical Coal Cleaning Processes, BOM/USDI Rept. J0166191, 153 pp.
45. Ergun, S. et al., Executive Summary, Op. Cit.
46. IGT Symposium Papers: Clean Fuels from Coal, Inst. Gas Tech., Chicago, 1973; 684 pp.
47. Mesko, J. E., "Coal Combustion in Limestone Beds", CEP Aug. 1978, p. 99.
48. Anon., "New Method Devised for Coal Desulfurization", C&E.N. September 25, 1978, p. 7.
49. Herlihy, J., Flue Gas Desulfurization in Power Plants, EPA Rept. pb 270295, Washington D.C., 1977.

50. Ergun, S. Op. Cit.
51. Hamersma, et al. "Meyers Process for Coal Desulfurization", in Wheelock, Op. Cit.
52. Ergun, S. Analysis of Technical and Economic Feasibility of Coal Cleaning by Physical and Chemical Methods. Nov 1977. LBL report to be published.
53. Cavallaro, J. A. et al., Sulfur Reduction Potential of U. S. Coals. USDI/BOM RI 8118, 1976.
54. Beekers, T. F., and R. E. C. Weaver, Coal Use in Louisiana. State of Louisiana Dept. of Natural Resources, Baton Rouge. 1978.
55. Mendizabal, Op. Cit.
56. Prepared from articles collected by D. Mobley, U. C. Berkeley.
57. Bartsch, R. & C. Tanelian, "Hydrogenation of Benzothiophene and Dibenzothiophene over Co-Mo-Al Catalyst", J Catal 35 (3), p. 353 (1974).
58. Hartough, H. D., Op. Cit.
59. Sittig, M., Sodium, Reinhold Pub. Co., New York, 1956. 529 pp.
60. Reggel, L., et al., "Desulfurization of Gasoline by Sodium", Fuel 55 p. 171 (1976).
61. Sittig, M., and A. S. Hawkes, Pet. Ref. 33 p. 193-6 (1954).
62. Loughrey, C. T., U. S. Patent 2039818 (April 24, 1936).
63. Vose, R. S., U. S. Patents 2055210, 2169545, and 2385431.
64. Sternberg, H. W. et al., "Reaction of Sodium with Dibenzothiophene", Ind. Eng. Chem. P. D. D. 13 (4), p. 433 (1974).
65. Morrison, R. T., and R. N. Boyd, Organic Chemistry, Allyn and Bacon, Inc., Boston 1966; 1200 pp.
66. Lazarov, L., and G. Angelova, "Treatment of Coals with Sodium in Liquid Ammonia Solution", Fuel 47, p. 333 (1968).
67. Ignasiak, B. S., and M. Gawlak, "Polymeric Structure of Coal", Fuel 56, p. 216 (1977).

68. Clegg, J. W. et al., Can. Oil and Gas Ind. 6 (12), 42-5 (1953).
69. Jacobs, M. B., Chemical Analysis of Air Pollutants, Intersci pub. N. Y. 1960, 430 pp.
70. Mendizabal, Op. Cit.
71. Schmid, B. K. and D. M. Jackson, Recycle SRC Processing, presented at 4th Int'l Conf. on Coal Gas., Liq., and Conv., Univ. of Pittsburgh, PA. Aug. 2-4, 1977.
72. Sternberg, Op. Cit.
73. Herschkowitz, F., work done towards completion of PhD thesis, U. C. Berkeley, 1978.
74. Streitweiser, A. L. and C. H. Heathcock, Org. Chem. MacMillan, N. Y. 1976, 1279 pp.
75. Schmid, B. K., and D. M. Jackson, The SRC II Process, 2nd Pacific Chem. Eng. Cong. (PACHEC '77).
76. Weast, R. C. Ed., "Values of Chemical Thermodynamic Properties", CRC Handbook, CRC Press Inc., Cleveland Ohio 1974.
77. Bienstock, D., et al., Sulfur Dioxide, USDI/BOM Information Circular 7836, 1958; 96 pp.
78. Washburn, E. W. et al., Eds., International Critical Tables, McGraw-Hill Inc., New York 1923 v. 3.
79. Haddon, S. T. and SH. G. Grayson, "Hydrocarbon Vapor-Liquid Equilibria", Pet. Ref. Sept. 1961.
80. Private Communication, George Preston, Flue Gas Div., EPRI, Palo Alto, CA 1978.
81. Anon., "Refined Product Prices", Oil and Gas J. Sept. 18, 1978.
82. Nekervis, W. F. and E. F. Hensley, Conceptual Design of a Commercial Scale Pilot Plant for Chemical Desulfurization of Coal, EPA Rept. 600-2/75-051, Sept. 1975.
83. Peters, M. S. and K. D. Timmerhaus, Plant Design and Economics for Chemical Engineers, McGraw-Hill Book Co., New York 1968.
84. Ergun, S., et al., An Analysis of Chemical Coal Cleaning Processes, U. S. BOM Contract J0166191, April 1977.
85. Anon., "New Clean Image for Coal", Env. Sci. and Tech. 11 (13) Dec. 1977.
86. Stambaugh, E. P., "Hydrothermal Coal Process", in Wheelock, Op. Cit.

This report was done with support from the Department of Energy. Any conclusions or opinions expressed in this report represent solely those of the author(s) and not necessarily those of The Regents of the University of California, the Lawrence Berkeley Laboratory or the Department of Energy.

Reference to a company or product name does not imply approval or recommendation of the product by the University of California or the U.S. Department of Energy to the exclusion of others that may be suitable.

TECHNICAL INFORMATION DEPARTMENT
LAWRENCE BERKELEY LABORATORY
UNIVERSITY OF CALIFORNIA
BERKELEY, CALIFORNIA 94720